Geochemistryy and geochronology of charnoenderbites in the Northern Marginal Zone of the Limpopo Belt, Southern Africa, and genetic models

Autor(en): **Berger, Michael / Kramers, Jan D. / Nägler, Thomas F.**

Objekttyp: **Article**

Zeitschrift: **Schweizerische mineralogische und petrographische Mitteilungen = Bulletin suisse de minéralogie et pétrographie**

Band (Jahr): **75 (1995)**

Heft 1

PDF erstellt am: **11.09.2024**

Persistenter Link: https://doi.org/10.5169/seals-57142

SCHWEIZ. MINERAL. PETROGR. MITT. 75, 17–42, 1995

Geochemistry and geochronology of charnoenderbites in the Northern Marginal Zone of the Limpopo Belt, Southern Africa, and genetic models

by *Michael Berger*[1], *Jan D. Kramers*[1] and *Thomas F. Nägler*[1]

Abstract

This paper presents petrological and geochemical data combined with zircon U–Pb dating and whole rock Nd model ages for the Northern Marginal Zone (NMZ), Zimbabwe. The granulite terrain of the NMZ comprises enderbites and charnockites as well as their retrograde equivalents. Field relationships and petrological data suggest that the enderbites and charnockites are primary igneous rocks, some of which have been deformed post intrusionally as a result of a ca. 2.6 Ga tectonic event that juxtaposed the NMZ granulites against the amphibolite facies granites and gneisses of the Zimbabwe Craton. Well defined trends of major and trace elements indicate fractionation of clinopyroxene, plagioclase and possibly orthopyroxene to be the mechanism for differentiation of these rocks. In addition, the NMZ has very similar geochemical characteristics to the Zimbabwe Craton, suggesting a close relationship between the two terrains. U-Pb-zircon dating yielded ages between ca 2.71 and 2.6 Ga for the intrusion of the charnoenderbites. Nd T_{DM} obtained on the same samples analysed for U–Pb on zircon, scatter closely around 3.0 Ga, giving differences between Nd-model ages and the intrusion ages of 360 to 420 Ma. Our data do not support terrane accretion or continental collision as a reason for Archean crustal thickening of the NMZ and charnoenderbite genesis, but they are in favour of a "soft" continent formation model.

Keywords: Archean, Granulites, geochemistry, zircon dating, Nd model ages, Limpopo Belt, Southern Africa.

Introduction

High grade metamorphic terrains occur in many Archean provinces, and the study of their relationship to medium to low grade granite greenstone terrains (cratons) is of interest because it may allow conclusions on Archean tectonic processes – were they similar to or different from those operating today? In this study we focus on the high grade Northern Marginal Zone of the Limpopo Belt in Southern Africa. This Archean high grade province is adjacent to the Zimbabwe Craton, which is a typical low grade Archean granite-greenstone terrain. The boundary between the two provinces is a thrust zone, which has been dated at 2.6 Ga (MKWELI et al., 1995). To explain the different histories of these two terrains a number of models have been proferred:

1. Terrane accretion (ROLLINSON, 1993): This assumes that the Northern Marginal Zone constitutes a "suspect" terrane accreted onto the Zimbabwe craton. Such a terrane would be expected to have its own distinct geochemical and isotope geochemical characteristics.

2. Isostatic uplift of primarily anomalously thick continental crust (RIDLEY, 1992); this model involves a zone of mantle downwelling to explain the crustal thickening by magmatic processes and the different geothermal gradients obtained for the craton and the Northern Marginal Zone.

3. Thickening by collision (the lack of proof of an opposing continent in the Archean does not mean this possibility has to be discounted).

These models can be tested (a) by studying the tectonic style of the boundary and its metamorphism, and (b) by petrogenetic and geo-

[1] Mineralogisch-Petrographisches Institut, Gruppe Isotopengeologie, Universität Bern, CH-3012 Bern, Switzerland.

chronological comparisons of units from the Northern Marginal Zone and the Zimbabwe Craton. While structural studies continue elsewhere (MKWELI, pers. comm.), this study is aimed at making a contribution in the second sense. We have carried out a petrographical and geochemical study of charnockites and enderbites of the Northern Marginal Zone and some associated rock types, as well as coupled zircon U–Pb and whole rock Sm–Nd work to compare intrusion ages with mean crustal residence times, specifically to address the following questions:

– Are the rocks of the Northern Marginal Zone exotic with reference to the Zimbabwe Craton, or could they represent a deeper level of the same or similar craton?

– Can the data support a terrane accretion model on the basis of ages and geochemical differences?

– Is there any evidence in the charnoenderbites of the Northern Marginal Zone (outside the clear influence of the 2.0 Ga event) of Archean Barrow-type prograde metamorphism, as would be expected in a collisional event, or are they of primary magmatic character?

Further we examine, as an alternative, a non-uniformitarian "soft" continent formation scenario such as proposed by CHOUKROUNE et al. (in press) and RIDLEY and KRAMERS (1990) in the light of the data.

Geological setting

The Limpopo Mobile Belt, situated between the Zimbabwe and Kaapvaal Archean cratons, is a tectonic province with a complex history of multiple tectonometamorphic events stretching in time from over 3 Ga to around 2 Ga (BARTON et al., 1990; KAMBER et al., 1995; BARTON et al., 1994). It consists of three zones of contrasting structural trends and patterns as well as lithology (COX et al., 1965; MASON, 1973): The Northern Marginal Zone (NMZ), the Central Zone (CZ) and the Southern Marginal Zone (SMZ; Fig. 1). The CZ is characterized by an at least 3.1 Ga old granulite grade supracrustal succession (BARTON et al., 1977), the Beit Bridge Group, and older tonalitic gneisses (the Sand River Gneisses). The late Archean history of the Central Zone involves the intrusion of the important Bulai Granitoid Suite at 2.57 Ga. (BARTON et al., 1994), comprising charnockites, enderbites and tonalitic to granodioritic rocks.

Seventy percent of the SMZ consists of charnoenderbitic gneisses and amphibolite facies equivalents. Supracrustal rocks, including ultramafic to mafic metavolcanics, quartz-magnetite lithologies, quartzites and metapelites, constitute the remainder. Zircons from an enderbite sample yielded an age of 2715 ± 5 Ma (RETIEF et al., 1990). The Matok intrusion is a late intrusive body which includes charnoenderbites as well as granitoids, for which zircon-ages between 2664 and 2671 Ma were determined (RETIEF et al., 1990; BARTON et al., 1992). All these ages for the SMZ have been interpreted as intrusion ages (ibid. and BOHLENDER et al., 1992).

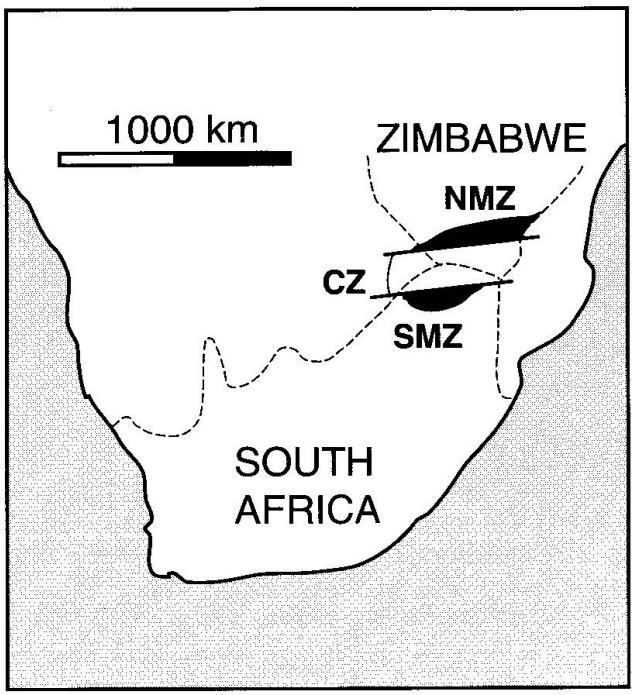

Fig. 1 Sketch map of Southern Africa showing the location of the Limpopo Belt and its 3 zones.

The NMZ is comparable to the SMZ, but is even more dominated by charnoenderbitic gneisses and their lower grade equivalents and contains fewer supracrustal rocks. Existing age determinations on NMZ rocks are discussed below and range from 2.9 to 2.6 Ga. In contrast to the CZ, both NMZ and SMZ have been interpreted as high grade metamorphic equivalents of the respective adjacent cratons (MASON, 1973; ROBERTSON and DU TOIT, 1981; VAN REENEN et al., 1988).

The three zones of the Limpopo Belt are separated from each other by major strike slip shear zones. These are the sinistral Palala Shear Zone on the CZ-SMZ transition, and the 2.0 Ga dextral Triangle-Tuli-Sabi Shear Zone on the NMZ-CZ boundary (MCCOURT and VEARNCOMBE, 1992; KAMBER et al., 1995). The contacts between Zimbabwe Craton – NMZ and between Kaapvaal Craton – SMZ are defined by two thrust sense

shear zones, the Umlali Thrust Zone in the north (JAMES, 1975; MKWELI et al., 1995) and the Hout River Shear Zone in the south (VAN REENEN et al., 1990).

Much research has concentrated in the past on the relations between the zones of the Limpopo Belt in order to construct tectonic models, that is, on their contrasting petrogenesis and geochronology, as well as on the nature of their contacts and the timing of the events that juxtaposed them (e.g., ROBERTSON, 1973a; COWARD, 1976; BARTON et al., 1992; MKWELI et al., 1995). Summaries are given by ROBERTSON and DU TOIT (1981) and ROERING et al. (1992). The timing of the various tectonic events is important: thrusting of the SMZ over the Kaapvaal Craton occurred at 2.67–2.7 Ga as documented by sheared and unsheared units within the Matok pluton (BARTON et al., 1992); post- and synorogenic granitoid intrusions in the NMZ-Zimbabwe Craton tectonic boundary constrain that thrusting event to 2.6–2.62 Ga (MKWELI et al., 1995); large-scale strike slip movement occurred under high grade, high pressure conditions between the NMZ and CZ at 2.0 Ga (KAMBER et al., 1995) along the Triangle Shear Zone. At least part of the high grade metamorphism visible in the CZ also appears to have occurred at that time (BARTON et al., 1994), although the CZ is largely made up of lithologies older than 3 Ga (e.g., BARTON et al., 1979; BARTON et al., 1990).

The evidence for major tectonism at 2.0 Ga invalidates the earlier models of an Archean (2.6–2.7 Ga) collision for the Limpopo Belt (ROERING et al., 1992; TRELOAR et al., 1992): models which lent much support to the view that plate tectonics operated in the same way in the Archean as at present (WINDLEY, 1993). Nevertheless, although the belt as a whole can no longer be used as an example of an Archean collision orogen, it contains areas which are highly suitable for studies of Archean metamorphism and tectonic styles. One of these is the NMZ.

The Northern Marginal Zone of the Limpopo Belt is 250 km long, WSW–ENE striking, and has a maximum width of 70 km across strike (Figs 2, 3). To the east the NMZ is cut by the mid-Proterozoic southern Mozambique Mobile Belt, while the westward continuation is partly obscured by Karoo basalts. The NMZ is juxtaposed to the Zimbabwe Craton along a major thrust-sense shear zone (JAMES, 1975; MKWELI et al., 1995). The NMZ consists mainly of enderbitic to charnockitic rocks which carry a more or less strongly developed gneissic fabric. To a much smaller extent ultramafic igneous rocks (metapyroxenites, metadunites or serpentinite), sometimes associated with magnetite-quartzites and/or rarely with metagabbros and metanorites do occur (ROBERTSON and DU TOIT, 1981). In the northern NMZ volumetrically large intrusions of syntectonic granites, referred to as the Razi Suite (ROBERTSON, 1973b), are important. These "granites", which also intrude the northern thrust, crystallized at least in part under granulite facies conditions, as is documented by the occurrence of orthopyroxene (MKWELI et al., 1995). The granites find their equivalent in the Kyle Granite Suite (ROBERTSON, 1973b) of the craton. A Rb/Sr errorchron age of 2883 ± 47 Ma was obtained by HICKMAN (1978; recalculated for $\lambda = 1.42 \times 10^{-11}$ y^{-1}) on 13 charnoenderbite and migmatite whole-rock samples from Bangala Dam in the eastern NMZ; this date was then interpreted as that of the high grade metamorphism. However, RIDLEY (1992) has argued that the charnoenderbites crystallized from a melt, rather than being the product of metamorphic recrystallization. A composite sample suite from the NMZ south of Buchwa, consisting of intrusive charnockites, granites, enderbites and retrogression zones in enderbites yielded a Rb/Sr errorchron age of 2583 ± 52 Ma with an initial $^{87}Sr/^{86}Sr$ ratio of 0.7047 ± 0.0007 (MKWELI et al., 1995) indicating some preceding crustal residence time. An aplitic dyke which cuts part of the NMZ-ZC thrust zone but is itself slightly deformed, has yielded a zircon U–Pb upper intercept age of 2627 ± 7 Ma (MKWELI et al., 1995), which confirms field evidence that this tectonism was approximately coeval with some of the Razi granite magmatism.

COWARD et al. (1976) separated two major deformational phases for the NMZ. The earliest phase is represented by a gneissic fabric, referred to as F1, in the charnoenderbites. This fabric has a relatively constant ENE–WSW trend and steep southerly dips. The deformation of the second phase, F2, occurred in broad anastomosing zones up to 1 km wide, in the centre of which narrow mylonite zones were developed. The fabric again has an ENE–WSW trend, but has moderate to steep dips. These zones enclose up to 5 km wide lenses of massive and homogeneous charnoenderbites (ODELL, 1975). In the southern NMZ the discrete shear zones become less abundant and massive and little deformed charnoenderbite bodies are batholith-like and can be traced along the strike of the NMZ over tens of kilometers. The F2 phase may well be coeval with the NMZ-CZ tectonism at 2.6 Ga.

The Zimbabwe Craton comprises granite-greenstone terrains ranging in age from 3.5 to 2.6 Ga (WILSON et al., 1978). The oldest of these is

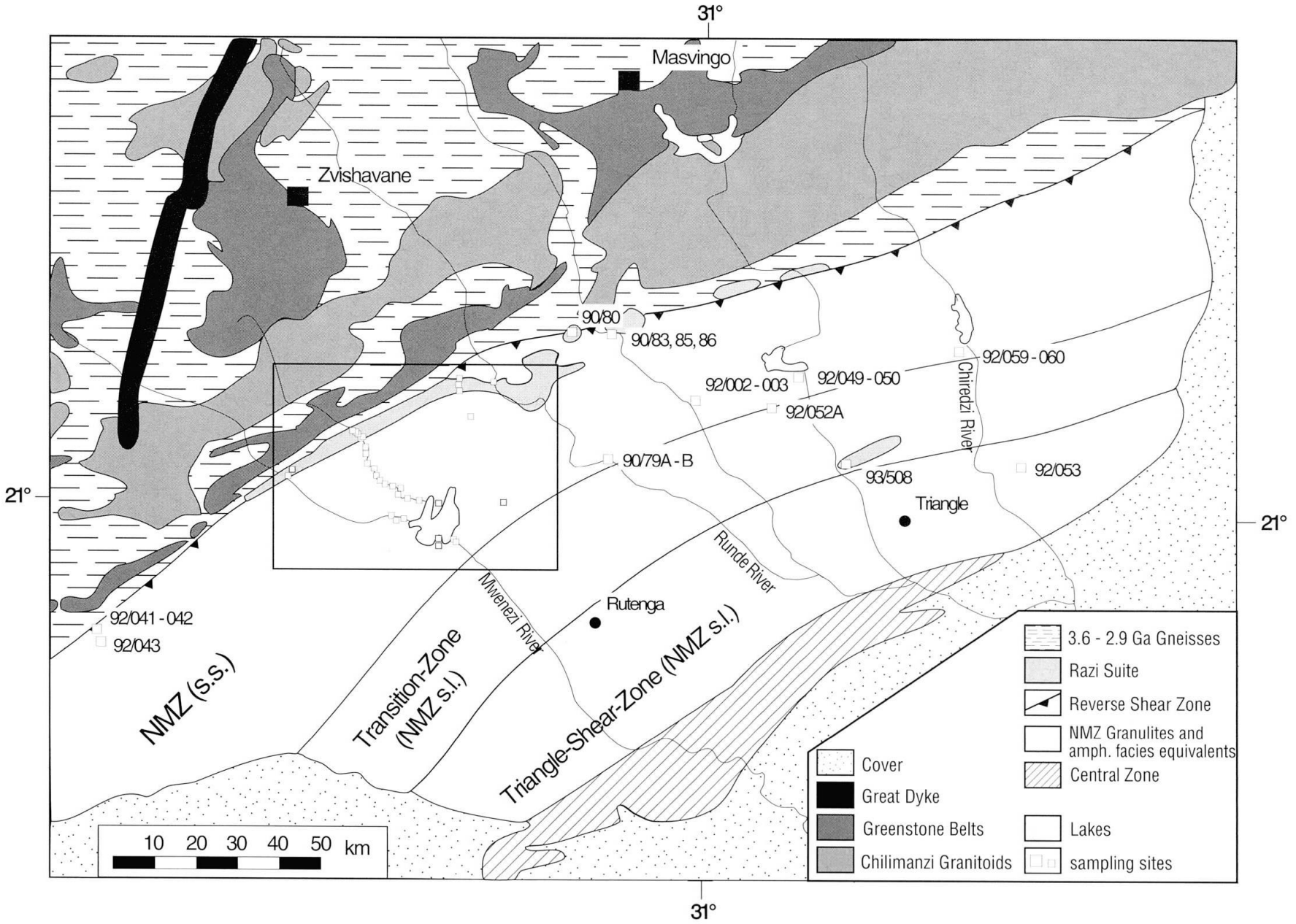

Fig. 2 Geological sketch map of the Northern Marginal Zone of the Limpopo Belt with sampling sites marked; redrawn after BLENKINSOP and ROLLINSON (1992).

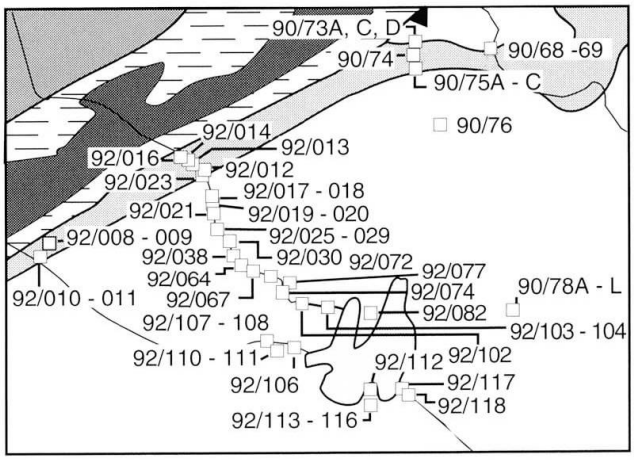

Fig. 3 Enlarged section of figure 2, including the sampling sites of the Mundi and Mwenezi river profile.

the Tokwe segment in the southern ZC which includes the ca. 3.5 Ga Tokwe River and Shabani gneisses (HAWKESWORTH et al., 1975; MOORBATH et al., 1977; TAYLOR et al., 1991). Tightly infolded within the gneisses are greenstone belt remnants (Sebakwian Group). This segment is interpreted as representative of the basement to the late Archean greenstone successions, the lower and the upper Bulawayan Group (2.9–2.6 Ga). Three further suites of mid- to late-Archean granitoids are distinguished: the ca. 2.9–2.8 Ga Chingezi Suite, the ca. 2.65–2.6 Ga Sesombi Suite and the ca. 2.6 Ga Chilimanzi Granite Suite (HAWKESWORTH et al., 1975; MOORBATH et al., 1976, 1977, 1986; TAYLOR et al., 1991). The emplacement of the widespread Chilimanzi Granite Suite was quasi contemporaneous with the thrust tectonism between the NMZ and the Zimbabwe craton. Within the Zimbabwe Craton, much of the deformation of greenstone belt sequences appears to be related to the intrusion of the late plutons, as characterized by JELSMA (1993) with the concept of "aureole tectonics". In the southern part of the ZC, adjacent to the NMZ, a trend, coparallel to the NNE–SSW trend of the NMZ gneisses, is developed. This fabric is caused by deformation along the thrust. Very important is the intrusion of the ca 2.5 Ga nearly N–S trending Great Dyke and its satellites (DAVIES et al., 1970; ROBERTSON and VAN BREEMEN, 1970) into both the craton and the north-western NMZ. This implies that both the craton and the NMZ must have been rigid at that time. In terms of lithology and the available age data, there is much support for the notion of earlier workers (MASON, 1973; ROBERTSON and DU TOIT, 1981) that the NMZ may represent the high grade equivalent of the Zimbabwe Craton.

Petrography of the charnoenderbitic suite and associated rocks

The dominant rock suite of the NMZ are the charnockites and enderbites (charnoenderbites). Contacts between enderbites and charnockites are magmatic, the latter being mostly intrusive into the former. Although magmatic contacts between different enderbites were not observable, the suite as a whole may represent a series of intrusions into similar rocks. The enderbites evidently lack a country rock of a different character into which they were intrusive. Within the charnoenderbites mafic granulites occur as small (decimeter) to large (kilometer) scale enclaves. These are never boudinaged, instead they are subangular bodies which often show an internal deformation fabric that is cut by the contact with charnoenderbite (Fig. 4a). The larger ones are often associated with ultramafics and banded quartz-magnetite rocks (meta supracrustals) and occasionally meta-pelites. The contacts of the charnoenderbites with these units, in the profile studied, are irregular and clearly magmatic. No evidence for a tectonic juxtaposition of these rocks has been found, nor been described by other authors so far.

The granites and charnockites of the Razi suite occur in the north and south of the NMZ as elongated batholiths, aligned along the regional NNE–SSW trend, and as leucosomes in migmatized enderbites. Particularly in the southern portion of the profile, granodiorites occur in cm to m wide zones and veins (see also section Geological setting, Fig. 4b) within the massive charnoenderbites. Their contacts to the country rock are diffuse and transitional, no magmatic contacts were observed (Fig. 4b). They appear to result from a localized retrogression/metasomatism, in part associated with the F2 deformation phase of COWARD et al. (1976).

The characterizations given below are based on the study of 74 samples of enderbite, charnockite, granite, retrogressive granodiorite, "granulite gneiss" and mafic granulite, taken from the Mundi/Mwenezi river profile and other selected localities (Figs 2 and 3). Mineral abbreviations follow KRETZ (1983).

The enderbites and charnockites are dark greenish to brown, medium grained rocks. Being the equivalents of tonalites and granites they consist of antiperthitic Plag, Qtz, Or/Mc (charnockites only), Bt, Opx (which is the main indication for granulite facies), minor green Hbl and sometimes Cpx, with accessory Ap, Zr, Fe-oxides (commonly Ilm) and Py. Bt-Qtz intergrowths, developed in almost every charnoenderbite sample,

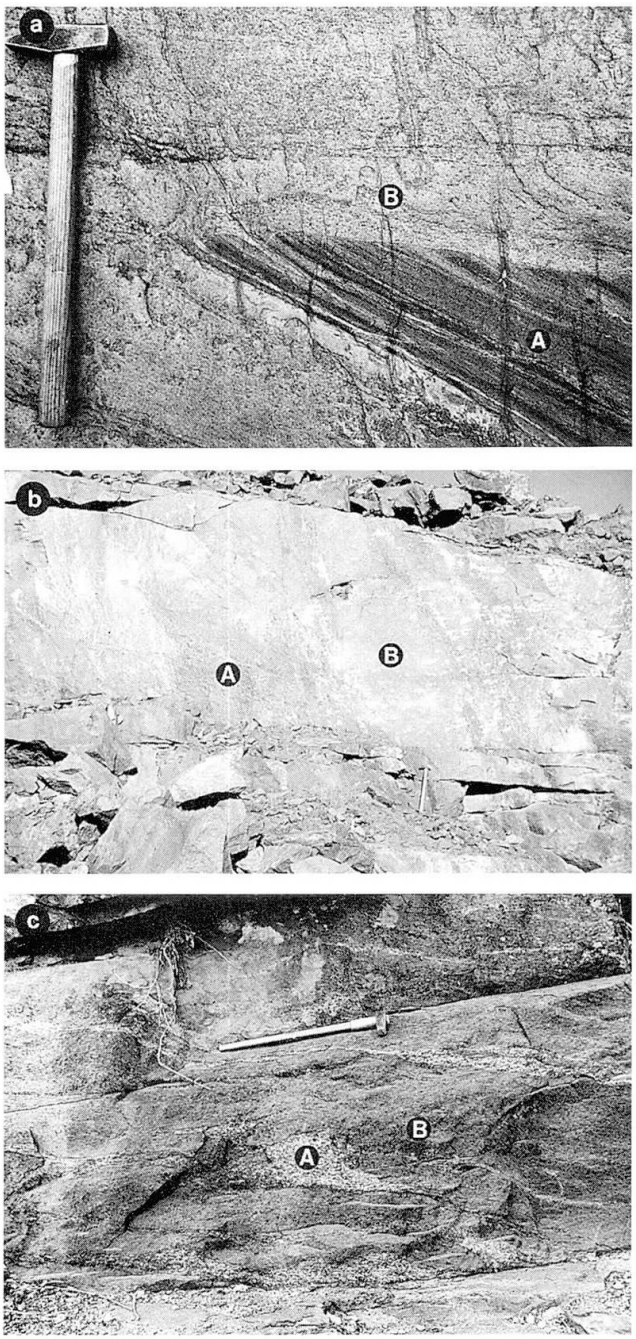

Fig. 4 a) Photograph showing a foliated mafic xenolith (A) within a partly retrogressed charnoenderbite (B). Picture taken in the Mwenezi river, north of Manyuchi Dam.
b) This outcrop picture, taken at Manyuchi Dam quarry (samples 92/113–116), illustrates the field-relationship between unaltered enderbite (A) and zones of retrogressive granodiorite (B). The retrograde zones and patches are irregularly distributed and are transitional to the enderbite domains.
c) Outcrop picture taken S of Musume Mission ca 8 km south of the Umlali thrust showing the partial melting relationship between a charnockitic leucosome (A) and an enderbitic paleosome (B).

have been interpreted by RIDLEY (1992) to be magmatic replacement textures of Opx. At Gwavamutangwi hill locality, ca 10 km west of sample locality 92/067, the charnoenderbites are Grt-bearing in a several ten meter domain along a magnetite-quartzite band. The occurrence of Grt in this case probably results from a magmatic assimilation of iron rich supracrustal material.

The charnoenderbites range from undeformed and massive, carrying granular, igneous textures to deformed, gneissic with a few samples displaying protomylonitic textures.

Where deformation produced a gneissic fabric, it took place at high T conditions as is documented by the grain-boundary migration of feldspar, and following recrystallization of Qtz, Plag and Ksp in microshears. In general little deformation is evident, except close to discrete, up to meter wide, shear zones.

At Musume mission locality (92/067), a late stage of the magmatic evolution, or rather the effect of high T conditions in the NMZ is observed: the granulite facies ("dry") melting of tonalitic enderbites has produced an Opx-bearing (charnockitic) melt in zones or patches and an Opx-Cpx-Plag restite (Fig. 4c). This locality is 13 km south of the northern thrust, and south of voluminous Razi-type charnockitic intrusions. The melting is therefore possibly related to the Razi-type granites and charnockites and will be discussed below (section Geochronology).

The granites of the Razi suite are coarse grained greyish to pinkish rocks, typically porphyric with centimeter sized Or. They consist of microperthitic Or, Mc, Plag, Qtz, Bt and ± green Hbl, with accessory Zr, Ap ± Rt and Fe-oxides.

The retrogression which produced the granodioritic zones is marked by the growth of Mc and Or at the cost of Plag along fluid pathways which appear in outcrop as decolourized zones within dark charnoenderbitic hostrock (Fig. 4b). The retrogressive granodiorites are medium to coarse grained rocks and are composed of Mc, Plag, microperthitic Or, Qtz, Bt and green Hbl, with accessoriy Zr, Ap and Fe-oxides.

A further type of retrogression which takes place throughout the NMZ is the replacement of pyroxene by green Hbl (Fig. 5a) or by Bt, which then grows as tiny ledges around Px (Fig. 5b; RIDLEY, 1992) with no macroscopic sign of metasomatism (no decolouration) as described for the granodiorites. This type of retrogression of charnoenderbitic rocks produces lithologies similar to the granulite gneisses of WORST (1962). This rock-type is still dark and charnoenderbitic in appearance. In the western NMZ towards Botswana,

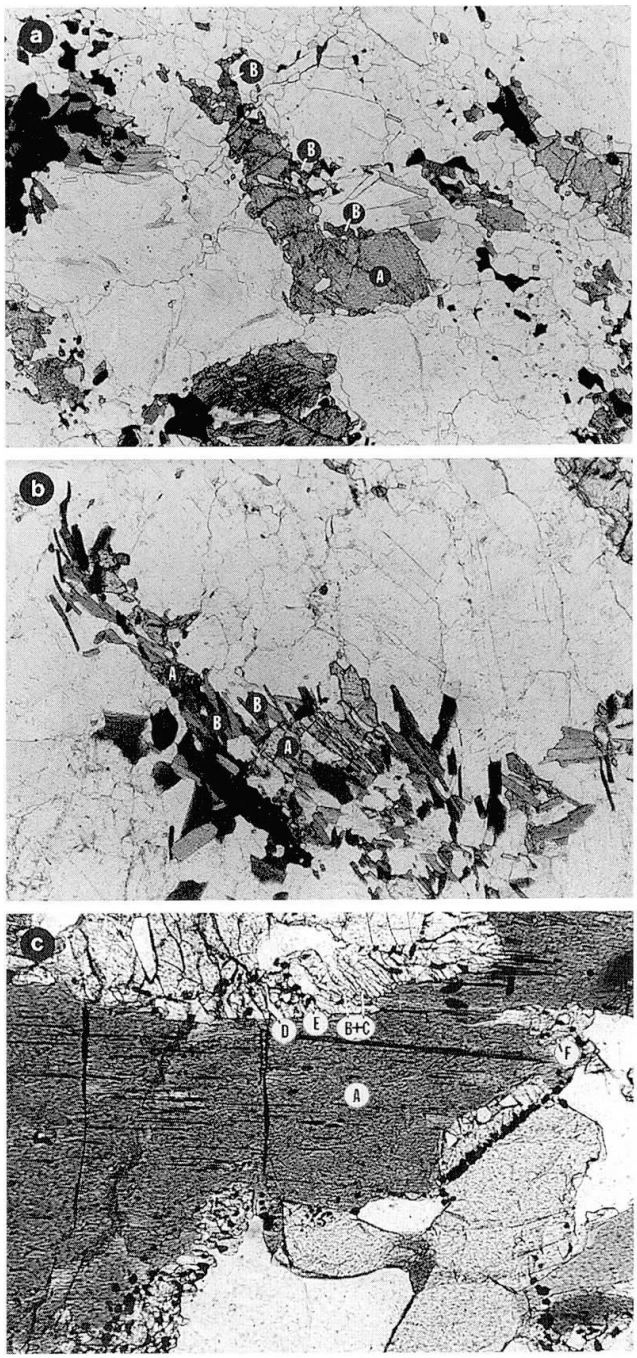

Fig. 5 a) Thin section of enderbite sample 92/038 from the Mundi river section, where Opx (A) is partially resorbed and replaced by green Hbl (B). Length of field: 6.25 mm.
b) Thin section of an enderbite sample 92/074. Tiny ledges of Bt (B) replace Opx (A). Length of field: 2 mm.
c) A mafic granulite (92/102) which was taken from a larger xenolith situated in a terrain of retrogressed charnoenderbite in the Mundi river section. Green brown primary Hbl (A) is replaced by a symplectite of Opx (B), ± Cpx (C), Qtz (D) and Mag (E). A green Hbl (F) partially replaces Px in the symplectite. Length of field: 1 mm.

orthopyroxene is totally absent in the gneisses and it remains unclear if granulite grade was ever reached in this area or if a complete retrogression of once higher grade rocks occurred (ROBERTSON and DU TOIT, 1981).

The mafic granulites are black fine to medium grained rocks that consist of Plag, Opx, Cpx, Hbl and minor Bt and Fe-oxides. Two different prograde reactions are observed in the mafic xenoliths that are incorporated in the charnoenderbites: (1) Px bearing, dehydrated rims in some amphibolite schollen within the charnoenderbites (ROLLINSON and BLENKINSOP, 1995) are interpreted to reflect the effect of the incorporation of these schollen in a water undersaturated melt.

(2) Pervasive dehydration reactions in mafic xenoliths as they occur throughout the NMZ within the charnoenderbites (Fig. 4a). Three samples of these rocks from two localities have been studied. All of them contain a primary Hbl which shows a prograde texture of symplectitic intergrown Opx ± Cpx and Qtz surrounding Hbl grains (Fig. 5c). Additionally an Fe-oxide phase occurs adjacent to or incorporated in the intergrowth zone (Fig. 5c). We interpret this texture to be the result of the following reaction:

Hbl = Opx ± Cpx (± Plag) + Qtz + Mag/Hem + H_2O.

Such textures only exist in the mafic xenoliths and not in the surrounding or adjacent charnoenderbites. This is taken as evidence, that the high P and T tectono-metamorphic conditions which caused partial melting of the charnoenderbites and their deformation and subsequent recrystallization (see above) led to a granulitization of the mafic xenolith, while the charnoenderbites persisted at the granulite grade.

SUMMARY

Whereas BOHLENDER et al. (1992) argued in the case of the SMZ for the existence of two different kinds of charnoenderbites, a magmatic and a metamorphic type, RIDLEY (1992) concluded that the NMZ charnoenderbite suite has a magmatic origin rather than a metamorphic one. Field work in the NMZ and petrography have provided evidence, that most charnoenderbites belong to a succession of intrusions in older, similar charnoenderbites, that are in a late stage remelted to form charnockites and granites. In contrast, no evidence was found which would support a metamorphic origin of the charnoenderbites.

Arrested charnockitization features such as they have been described for some Indian charnockite localities (e.g., RAITH and SRIKANTAPPA,

1993) and which point to a granulitization during near-isothermal uplift by locally derived carbonic fluids, have also never been observed in either of the Marginal Zones of the Limpopo Belt.

Geochemistry

On the basis of field relations and petrography the rocks studied can be divided into 6 distinctive groups (as discussed above). Samples are subdivided into these lithological groups irrespective of area, with the exception of those from the Sarahuru locality, singled out to illustrate trends within an individual charnoenderbitic body. The identification of geochemical trends may be used as a test for a magmatic origin. If fractionation processes suggested by the major elements in a magmatic scenario coincide with those suggested by trace elements, and if the trends for one distinct pluton are further unambiguously the same as for the whole NMZ rock suite, then the suite should be regarded as magmatic. We also investigate if geochemistry can be used to distinguish between a magma evolution in the Px- or Hbl-stability field. Further, the data from the NMZ are compared with data from three clearly magmatic suites in the Zimbabwe Craton, the ca. 2.9–2.8 Ga Chingezi- and Mashaba tonalites, the Chinamora gneissic granites and the ca 2.6 Ga Chilimanzi Suite granites (Chinamora granites) (data taken from LUAIS and HAWKESWORTH, 1994 and from SNOWDEN and SNOWDEN, 1981). These are lithologically rather similar to the NMZ charnoenderbite suite, although with granitoid rather than charnoenderbitic assemblages.

ANALYTICAL METHODS

XRF analyses of 74 samples from the NMZ (sites marked on Figs 2 and 3) were performed at the universities of Fribourg and Lausanne. For the major element measurements glass discs were made by fusing a mixture of rock powder with Li-tetraborate and Li-fluoride. The XRFS analysis of trace elements were obtained on powder pellets of 10 g rockpowder and 1 ml of a solution of 3.6 wt% SiO_2, 6.4 wt% KCO_3 and 90 wt% H_2O. The chemical compositions are listed in tables 1a to 1f.

MAJOR ELEMENT CHEMISTRY

All the major element data show relatively uniform trends if plotted vs SiO_2, although a wider variation of K_2O/SiO_2 and Na_2O/SiO_2 ratios compared to the ratios of divalent ions to SiO_2 is visible. In a ternary diagram of K_2O, Na_2O and CaO (Fig. 6) the trend for the less evolved lithologies is characterized by a general increase in K_2O and Na_2O, whereas the more differentiated rocks show increasing K_2O. Also obvious is the good agreement with the data for the tonalites and the Chilimanzi granites from the craton. The trend described by the NMZ lithologies is best explained by a fractionation of mainly Cpx and/or Hbl for the enderbites (accompanied by an increasing amount of plagioclase fractionation) and of Plag ± Cpx/Hbl for the more evolved members of the suite. Addition of K-rich fluids, as also suggested by the field and textural evidence, is probably the main control on the vertical trend defined by the retrograde rocks in figure 6. In Harker diagrams MgO, CaO, Fe_2O_3, TiO_2 and MnO show decreasing trends with increasing silica (Figs 7a–e). These patterns may be explained by a fractionation of Px/Hbl, Bt, Plag and possibly minor phases such as Ilm. The decrease of Al_2O_3 with increasing SiO_2 for the main field of the NMZ lithologies, also shown by the samples from the Sarahuru locality (Fig. 7f), is in part a straightforward dilution feature but may indicate Plag fractionation, as also suggested by the ternary diagram of K_2O, Na_2O and CaO (Fig. 6). Na_2O defines a wider, boomerang-shaped field for the cratonic as well as for the NMZ-rock suite, with Na_2O increasing at first in the less evolved enderbites (cratonic tonalites and Chinamora gneisses) and then a decreasing trend with increasing SiO_2 for the more differentiated rock types (Razi-type granites and charnockites, Chilimanzi granites; figure 7g). In good agreement with this pattern is a fractionation of Cpx (major) and Plag (minor?) for the ascending trend and mainly Plag fractionation for the descending trend. K_2O/SiO_2 ratios display a wide range for the enderbites, although K_2O generally increases with increasing SiO_2 as is shown by the Sarahuru samples (Fig. 7h). Again, the cratonic tonalites display a general conformity with the NMZ lithologies. The wider variation in Na_2O and K_2O is exactly what we would expect for a suite of cogenetic batholiths which varied in their water activity and in the pressure regime during crystallization, as suggested by the results of BOHLEN et al. (1983) and SECK (1971).

The MnO–MgO plot (Fig. 8) can be used to distinguish Cpx and Opx fractionation from Hbl and Bt fractionation, as the fractionation vectors of Cpx/Opx and Hbl/Bt (calculated using microprobe data on phases from NMZ lithologies, vectors valid for MgO contents of less then ca 2.5 wt%) are sufficiently different. This is a tool to

Tab. 1a Major- and trace-element analyses on rocks from the NMZ, Limpopo Bet Zimbabwe.

sample No		90/78A	90/78B	90/78C	90/78D	90/78E	90/78F	90/78G	90/78H	90/78K	90/78L	90/68	90/73A	90/73c	90/73D	90/74	90/75A
lithology		rg	rg	rg	e	e	e	e	rg	rg	rg	rg	gg	gg	gg	mx	gg
SiO_2	(wt%)	74.2	74.38	73.59	70.52	71.06	71.8	66.26	72.47	73.54	72.04	74.09	70.71	70.16	67.59	57.78	75.14
TiO_2	(wt%)	0.06	0.06	0.07	0.3	0.23	0.28	0.41	0.21	0.12	0.17	0.05	0.23	0.13	0.36	1.37	0.06
Al_2O_3	(wt%)	13.9	13.84	14.01	14.84	14.57	14.62	16.52	14.15	13.86	14.72	13.79	14.88	14.96	15.56	15.95	13.26
Fe_2O_3	(wt%)	0.53	0.63	1.02	3.2	3.01	2.46	4.35	1.49	1.1	1.46	0.41	2.22	2.71	4.02	7.69	0.35
MnO	(wt%)	0.01	0.01	0.01	0.05	0.04	0.04	0.05	0.02	0.02	0.01	0	0.03	0.06	0.06	0.09	0.01
MgO	(wt%)	0.01	0.03	0.07	0.68	0.64	0.45	0.93	0.38	0.16	0.28	0	0.66	0.87	1.07	2.07	0.01
CaO	(wt%)	1.1	1.17	1.1	2.95	2.65	2.33	3.58	1.61	1.31	2.06	0.69	2.98	3.86	4	4.7	1.5
Na_2O	(wt%)	3.32	3.44	2.97	4.19	4.01	3.68	4.53	3.15	2.78	3.61	2.74	3.05	3.63	3.8	3.21	1.94
K_2O	(wt%)	5.35	5.24	5.21	0.98	1.55	2.77	1.06	4.18	4.95	3.24	5.87	2.97	1.12	1.12	3.3	5.26
P_2O_5	(wt%)	0.02	0.01	0	0.04	0.02	0.02	0.08	0.04	0.02	0.02	0.01	0.05	0.05	0.12	0.57	0
H_2O (total)	(wt%)	0.38	0.11	0.12	0.27	0.26	0.21	0.31	0.29	0.33	0.34	0.23	0.32	0.44	0.43	0.35	0.29
Total	(wt%)	98.88	98.92	98.17	98.02	98.04	98.66	98.08	97.99	98.19	97.95	97.88	98.1	97.99	98.13	97.08	97.82
Ba	(ppm)	825	689	349	19	150	394	< 3	473	722	847	687	747	126	47	1684	3863
Cr	(ppm)	< 3	< 3	< 3	8	5	4	12	3	< 3	6	< 3	6	12	15	23	< 3
Cu	(ppm)	< 4	< 4	< 4	< 4	< 4	< 4	< 4	< 4	< 4	< 4	< 4	< 4	< 4	< 4	17	< 4
Ga	(ppm)	17	17	21	20	20	19	24	18	16	19	15	16	17	19	22	13
Nb	(ppm)	< 5	< 5	< 5	< 5	< 5	< 5	5	7	< 5	< 5	< 5	< 5	< 5	< 5	17	< 5
Ni	(ppm)	4	< 2	< 2	5	< 2	6	4	5	4	< 2	4	< 2	< 2	5	12	4
Pb	(ppm)	40	43	47	24	24	32	27	39	39	30	43	28	27	14	26	30
Rb	(ppm)	127	120	121	14	29	61	25	121	130	72	179	84	31	51	89	107
Sr	(ppm)	164	160	105	170	202	152	194	134	136	261	104	214	212	194	562	484
Th	(ppm)	< 1	1	4	37	21	23	34	11	7	4	< 1	46	94	11	26	5
V	(ppm)	3	< 3	< 3	15	16	11	21	9	4	7	< 3	16	10	29	100	9
Y	(ppm)	< 1	4	13	15	11	8	19	17	17	4	< 1	4	8	4	36	< 1
Zn	(ppm)	11	9	22	55	52	39	71	30	19	25	5	33	45	63	120	2
Zr	(ppm)	88	56	63	166	177	132	232	154	80	108	40	165	174	177	639	32
U	(ppm)	3	5.2	7.6	4.6	4.8	3.2	3.7	12.1	8.8	2.5	3.1	2.7	3.2	2.4	1.6	3

e = enderbite, c = charnockite, rg = retrogressive granodiorite, g = granite, gg = granulite gneiss, mx = mafic xenolith.

Tab. 1b Major- and trace-element analyses on rocks from the NMZ, Limpopo Belt Zimbabwe.

sample No		90/75B	90/75C	90/76	90/79A	90/79B	90/80	90/83	90/85	90/86	92/002	92/003	92/008	92/010	92/011	92/012
lithology		e	c	c	c	rg	g	g	g	g	e	e	g	c	c	g
SiO_2	(wt%)	67.86	71.57	71.76	70.59	74.49	72.05	72.14	72.08	71.7	58.7	72.07	74.11	75.24	75.77	69.75
TiO_2	(wt%)	0.43	0.21	0.26	0.36	0.04	0.26	0.26	0.17	0.3	0.76	0.22	0.08	0.05	0.06	0.42
Al_2O_3	(wt%)	14.87	14	14.24	14.67	14.07	14.48	14.29	14.26	14.32	18.88	15.38	14.51	13.47	13.52	14.98
Fe_2O_3	(wt%)	3.85	2.47	2.47	3	0.35	1.86	1.57	1.69	2.17	5.98	1.47	0.75	0.38	0.34	3.37
MnO	(wt%)	0.03	0.03	0.04	0.03	0.01	0.03	0.02	0.02	0.03	0.09	0.02	0.02	0.02	0.01	0.02
MgO	(wt%)	1.52	0.73	0.79	0.62	0	0.43	0.47	0.27	0.49	3	0.41	0.09	0.16	0.09	0.53
CaO	(wt%)	3.52	2.46	2.04	2.67	1.5	1.69	1.38	1.24	1.71	7.12	2.36	1.04	1.68	0.71	1.22
Na_2O	(wt%)	3.18	2.77	4.15	3.33	2.93	3.28	3.25	2.94	3.46	4.16	5.24	3.57	3.28	2.99	2.93
K_2O	(wt%)	2.24	3.53	2.02	2.56	4.44	3.94	4.06	4.74	4.08	0.76	2.43	5.9	5.1	6.39	6.78
P_2O_5	(wt%)	0.12	0.07	0.03	0.07	0	0.08	0.05	0.04	0.07	0.17	0.04	0.01	0.01	0.02	0.14
H_2O (total)	(wt%)	0.36	0.34	0.24	0.34	0.35	0.14	0.49	0.35	0.43	0.57	0.65	0.38	0.64	0.27	0.25
Total	(wt%)	97.99	98.18	98.04	98.24	98.18	98.24	97.98	97.8	98.76	100.18	100.26	100.45	100.03	100.17	100.38
Ba	(ppm)	1771	843	349	1094	1127	685	760	851	1129	445	582	896	461	742	2123
Cr	(ppm)	33	14	6	6	< 3	5	7	< 3	7	60	11	13	15	12	11
Cu	(ppm)	21	< 4	< 4	13	< 4	< 4	< 4	< 4	10	43	8	9	18	13	12
Ga	(ppm)	18	15	18	17	13	18	17	17	18	24	18	15	13	12	16
Nb	(ppm)	< 5	< 5	< 5	< 5	< 5	< 5	< 5	< 5	< 5	5	1	1	1	1	1
Ni	(ppm)	23	8	5	5	4	6	7	6	< 2	57	9	9	11	8	9
Pb	(ppm)	13	16	13	21	36	37	33	52	34	1	21	38	31	35	28
Rb	(ppm)	53	78	30	66	103	127	93	110	92	4	37	144	149	198	124
Sr	(ppm)	533	294	315	183	177	218	171	190	245	313	257	114	85	121	257
Th	(ppm)	5	< 1	< 1	45	< 1	25	32	55	48	1	13	9	1	1	1
V	(ppm)	53	31	18	21	< 3	12	13	10	21	137	14	7	7	4	16
Y	(ppm)	6	< 1	< 1	11	30	11	8	9	7	19	6	2	4	1	9
Zn	(ppm)	58	30	39	44	5	33	27	31	35	65	35	1 1,	6	6	44
Zr	(ppm)	165	114	87	281	46	151	165	283	236	144	141	64	34	19	309
U	(ppm)	2.2	1.9	1.3	3.5	15.8	4	4	4.2	2.1	1.3	3.1	3.2	3.3	3.5	2.3

e = enderbite, c = charnockite, rg = retrogressive granodiorite, g = granite, gg = granulite gneiss, mx = mafic xenolith.

Tab. 1c Major- and trace-element analyses on rocks from the NMZ, Limpopo Belt Zimbabwe.

sample No		92/013	92/014	92/016	92/017	92/018	92/019	92/020	92/021	92/023	92/025	92/027	92/029	92/030	92/038
lithology		c	c	c	rg	c	c	rg	c	c	e	e	e	c	e
SiO_2	(wt%)	67.17	70.58	70.43	75.77	71.5	73.38	73.31	72.67	64.84	75.72	70.12	60.99	74.6	65.61
TiO_2	(wt%)	0.75	0.41	0.42	0.1	0.41	0.15	0.16	0.19	0.84	0.07	0.29	0.62	0.13	1.11
Al_2O_3	(wt%)	15.28	14.83	14.76	13.08	14.43	14.16	14.35	14.38	16.23	14.7	15.77	15.39	14.09	13.77
Fe_2O_3	(wt%)	4.12	2.77	3.07	0.64	3.16	1.44	1.38	1.62	4.43	0.45	2.45	9.67	1.34	6.75
MnO	(wt%)	0.05	0.03	0.04	0.02	0.05	0.05	0.02	0.02	0.06	0.01	0.04	0.11	0.02	0.1
MgO	(wt%)	1.01	0.87	1.06	0.27	0.97	0.39	0.35	0.54	1.28	0.32	0.67	4.92	0.38	1.56
CaO	(wt%)	2.58	2.24	2.18	1.56	3.04	1.62	1.82	1.93	3.29	3.73	2.66	5.06	1.76	3.73
Na_2O	(wt%)	3.37	3.35	3.44	2.58	4.06	3.46	4.32	3.19	3.9	4.29	5.35	2.95	3.72	3.35
K_2O	(wt%)	5.4	4.68	4.56	5.04	2.09	4.89	4.2	4.97	4.55	0.81	2.37	0.84	4.04	3.65
P_2O_5	(wt%)	0.25	0.13	0.13	0.01	0.09	0.04	0.04	0.04	0.31	0.01	0.08	0.19	0.02	0.24
H_2O (total)	(wt%)	0.45	0.45	0.33	0.98	0.54	0.25	0.39	0.31	0.15	0.41	0.36	0.1	0.2	0.26
Total	(wt%)	100.43	100.32	100.42	100.06	100.33	99.82	100.34	99.85	99.87	100.5	100.15	100.84	100.31	100.13
Ba	(ppm)	1773	1425	1106	3881	874	1130	1095	2010	1618	423	488	403	1110	981
Cr	(ppm)	20	20	29	7	18	13	12	16	16	4	19	159	10	31
Cu	(ppm)	12	14	14	13	17	14	12	13	17	10	11	119	11	20
Ga	(ppm)	18	16	16	14	18	16	18	15	20	15	19	18	16	22
Nb	(ppm)	15	5	5	1	6	2	1	1	14	1	6	5	2	19
Ni	(ppm)	13	16	18	12	15	11	10	13	12	8	15	129	11	23
Pb	(ppm)	27	25	25	17	18	35	38	22	21	15	26	1	32	8
Rb	(ppm)	131	102	108	112	34	137	59	98	106	6	49	20	109	115
Sr	(ppm)	315	293	300	413	237	181	172	359	447	286	267	161	198	287
Th	(ppm)	11	69	58	1	1	23	33	1	12	3	9	1	17	
V	(ppm)	41	27	34	14	37	15	12	31	41	8	25	114	19	72
Y	(ppm)	25	5	11	1	8	3	6	2	24	1	9	12	2	36
Zn	(ppm)	60	38	48	11	44	22	27	22	61	9	47	40	22	87
Zr	(ppm)	383	227	188	46	168	121	136	131	385	48	143	143	105	310
U	(ppm)	2.5	3.8	3.1	1.4	1.2	2.4	2.3	1.3	2.4	1.2	2.7	1.7	3.3	3.1

e = enderbite, c = charnockite, rg = retrogressive granodiorite, g = granite, gg = granulite gneiss, mx = mafic xenolith.

Tab. 1d Major- and trace-element analyses on rocks from the NMZ Limpopo Belt Zimbabwe.

sample No		92/041	92/042	92/043	92/049	92/050	92/052A	92/053	92/059	92/060	92/064	92/067	92/072	92/074	92/077
lithology		g	rg	e	e	e	e	e	c	e	g	e	e	e	e
SiO_2	(wt%)	74.29	70.51	67.13	70.29	71.15	62.58	74.73	75.28	63.47	63.94	62.83	64.03	66.62	65.92
TiO_2	(wt%)	0.09	0.24	0.65	0.32	0.28	0.58	0.18	0.03	0.52	1.35	1.46	0.69	0.43	0.56
Al_2O_3	(wt%)	14.74	15.63	15.46	15.59	15.33	17.22	13.71	15.2	17.19	14.72	16.45	16.71	16.46	16.94
Fe_2O_3	(wt%)	0.57	1.16	4.78	3.08	2.74	5.95	1.43	0.19	5.32	6.86	5.74	5.16	4.37	4.51
MnO	(wt%)	0.01	0.01	0.05	0.06	0.05	0.07	0.02	0.01	0.07	0.08	0.05	0.06	0.06	0.05
MgO	(wt%)	0.17	0.24	1.6	0.96	0.83	2.78	0.46	0.12	2.81	2.15	1.62	2.3	1.43	1.39
CaO	(wt%)	1.6	1.57	3.95	3.41	2.96	5.52	2.25	3.87	5.54	3.74	4.17	4.94	4.11	4.7
Na_2O	(wt%)	3.08	3.04	4.36	4.81	4.84	4.13	3.87	4.09	4.24	4.12	4.73	4.39	4.81	4.53
K_2O	(wt%)	5.78	6.89	1.68	1.22	1.5	0.85	2.81	1.35	1	2.33	1.65	1.12	1.2	0.95
P_2O_5	(wt%)	0.01	0.18	0.19	0.06	0.04	0.15	0.03	0.01	0.12	0.52	0.49	0.19	0.16	0.15
H_2O (total)	(wt%)	0.09	0.54	0.57	0.31	0.38	0.18	0.46	0.1	0.14	0.37	0.53	0.33	0.45	0.62
Total	(wt%)	100.42	100.01	100.42	100.11	100.11	100	99.92	100.22	100.42	100.18	99.72	99.93	100.11	100.34
Ba	(ppm)	2076	2967	578	177	257	507	756	1145	582	689	819	1711	431	316
Cr	(ppm)	3	2	11	21	12	60	11	8	65	49	19	54	19	20
Cu	(ppm)	8	13	25	12	12	21	10	14	28	24	61	41	11	26
Ga	(ppm)	13	15	21	20	20	20	15	13	20	26	26	20	21	21
Nb	(ppm)	1	1	5	9	14	4	4	1	3	39	12	5	8	8
Ni	(ppm)	8	10	15	14	13	34	11	7	45	35	24	31	14	17
Pb	(ppm)	19	71	9	22	26	1	20	13	1	11	10	1	11	3
Rb	(ppm)	96	139	22	24	29	14	95	21	11	135	36	16	11	4
Sr	(ppm)	375	367	276	167	163	340	113	269	290	277	687	599	235	291
Th	(ppm)	1	366	1	21	42	7	26	1	1	5	17	1	13	
V	(ppm)	12	17	58	26	19	92	7	8	96	58	85	74	39	53
Y	(ppm)	1	10	6	14	20	10	6	1	9	81	23	11	17	11
Zn	(ppm)	9	11	51	52	57	71	21	8	50	112	84	67	61	48
Zr	(ppm)	88	129	119	149	141	105	122	13	96	422	425	186	200	211
U	(ppm)	1.8	0.9	1.9	3.6	6.3	2.3	4.2	1.7	1.7	3	3.8	1.4	2.3	2.5

e = enderbite, c = charnockite, rg = retrogressive granodiorite, g = granite, gg = granulite gneiss, mx = mafic xenolith.

Tab. 1e Major- and trace-element analyses on rocks from the NMZ, Limpopo Belt Zimbabwe.

sample No		92/082	92/102	92/103	92/104	92/106	92/109	92/110	92/111	92/112	92/113	92/114	92/115	92/116	92/117	92/118
lithology		rg	mx	c	e	rg	e	c	e	g	e	e	rg	rg	e	rg
SiO_2	(wt%)	74.97	51.04	69.47	65.57	75.79	70.37	73.86	70.35	73.31	66.54	65.81	72.16	75.07	70.36	74.23
TiO_2	(wt%)	0.19	0.82	0.34	0.36	0.12	0.32	0.18	0.3	0.22	0.55	0.55	0.21	0.17	0.43	0.22
Al_2O_3	(wt%)	13.3	14.09	15.97	14.19	13.47	15.35	14.12	15.37	14.05	16.62	16.44	14.95	13.45	14.66	13.64
Fe_2O_3	(wt%)	0.64	12.23	2.7	6	1.01	3.95	1.66	3.89	2.03	4	4.68	1.89	1	3.69	1.5
MnO	(wt%)	0.01	0.18	0.03	0.11	0.02	0.06	0.02	0.05	0.03	0.05	0.07	0.02	0.01	0.07	0.01
MgO	(wt%)	0.16	8.71	0.99	4.95	0.26	0.87	0.46	0.78	0.38	1.29	1.29	0.43	0.34	1.53	0.38
CaO	(wt%)	0.99	10.17	3.58	4.35	1.66	3.82	2.14	3.66	1.75	3.76	3.81	2.23	1.48	2.88	1.66
Na_2O	(wt%)	2.94	2.21	4.43	3.57	3.55	4.45	3.27	4.47	3.53	4.93	5.15	3.96	3.15	4.59	3.39
K_2O	(wt%)	5.93	0.17	1.86	0.96	4.12	1.01	4.37	0.99	4.56	1.68	1.47	3.82	4.97	1.5	4.42
P_2O_5	(wt%)	0.01	0.1	0.08	0.07	0.01	0.09	0.03	0.09	0.07	0.15	0.14	0.04	0.02	0.11	0.04
H_2O (total)	(wt%)	0.64	0.25	0.43	0.41	0.36	0.03	0.03	0.16	0.5	0.29	0.32	0.53	0.33	0.48	0.42
Total	(wt%)	99.78	99.99	99.89	100.54	100.37	100.33	100.13	100.11	100.42	99.87	99.73	100.23	100	100.29	99.9
Ba	(ppm)	1023	31	772	602	796	270	2706	371	1064	280	332	1026	1440	193	956
Cr	(ppm)	10	256	20	301	9	14	12	12	10	25	26	18	11	39	13
Cu	(ppm)	13	24	8	17	10	10	12	11	12	12	13	10	9	28	11
Ga	(ppm)	15	16	20	22	15	21	14	20	18	24	24	18	14	22	15
Nb	(ppm)	6	1	8	8	3	5	1	11	5	12	11	3	1	21	5
Ni	(ppm)	7	126	12	112	8	12	11	8	10	16	14	8	9	26	8
Pb	(ppm)	32	1	14	2	34	15	17	7	37	12	11	28	22	18	27
Rb	(ppm)	152	1	32	33	91	10	72	35	156	51	33	88	124	65	106
Sr	(ppm)	108	96	287	195	104	190	262	179	145	199	214	186	167	145	139
Th	(ppm)	22	1	3	3	9	1	1	8	28	12	1	41	25	14	20
V	(ppm)	2	230	26	64	10	32	26	15	24	42	55	16	11	61	15
Y	(ppm)	3	40	6	19	9	12	1	20	11	11	14	3	3	45	3
Zn	(ppm)	12	90	43	98	17	62	24	57	34	71	78	33	19	67	25
Zr	(ppm)	99	87	153	146	89	126	129	142	113	280	304	171	136	112	106
U	(ppm)	2.6	1.8	1.7	3.4	3.1	1.8	1.6	1.7	3	2.4	3.3	4.5	2.9	11.7	3.3

e = enderbite, c = charnockite, rg = retrogressive granodiorite, g = granite, gg = granulite gneiss, mx = mafic xenolith.

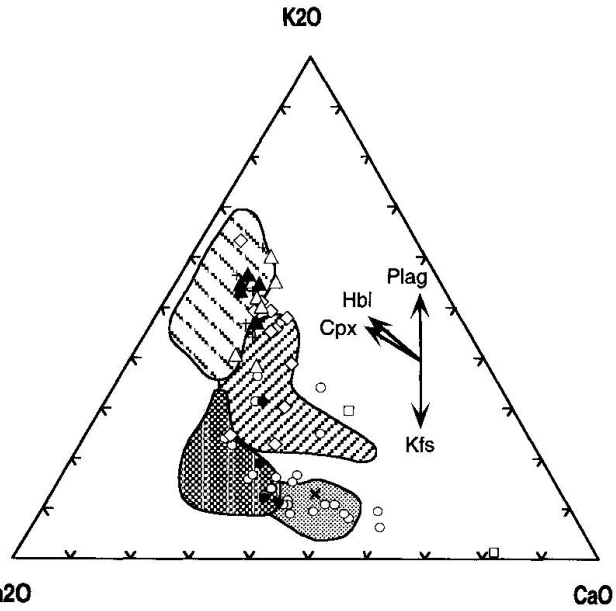

Fig. 6 K_2O–Na_2O–CaO diagram (oxides in weight %) for the NMZ lithologies, included are 4 different lithologies from the ZC; circles: enderbites, squares: mafic xenoliths, rhombs: charnockites including Razi Suite charnockites, plus-symbols: granites, triangles: retrogressive lithologies, x-symbols: granulite gneisses, filled symbols: samples from one distinct batholith (Sarahuru-quarry); lightly dotted area: Chingezi and Mashaba tonalites type I, densely dotted area: Chingezi and Mashaba tonalites type II (data taken from LUAIS and HAWKESWORTH, 1994), dense right-vergent lines: Chinamora gneissic granites, left-vergent lines: Chinamora granites (Chilimanzi-Suite; data taken from SNOWDEN and SNOWDEN, 1981). For further explanations see text. Fractionation vectors are calculated using microprobe data on phases from NMZ lithologies.

identify magma differentiation in the Opx-Cpx or Hbl-Bt stability field. The white arrow illustrates the suggested trend of differenciation for the NMZ charnoenderbites which correlates quite well with a fractionation of Cpx and Opx. Obvious is, that the trends of the Chinamora gneissic granites and the Chingezi and Mashaba tonalites type I (LUAIS and HAWKESWORTH, 1994) do not correlate with Cpx/Opx fractionation, suggesting that they rather evolved in the Hbl/Bt stability field. Surprisingly, the trend for the Chilimanzi granites and the trend for the Chingezi and Mashaba tonalites type II, interpreted by LUAIS and HAWKESWORTH (1994) to represent the products of two stages of partial melting and a subsequent fractional crystallization, also correlate with the fractionation trends of Cpx and Opx in this plot.

TRACE ELEMENT CHEMISTRY

Logarithmic plots of LIL-elements and included fractionation vectors for phases such as Hbl, Cpx, Plag, Bt and Kfs are used to check and further evaluate magmatic fractionation processes as they have been suggested by the major element behaviour. The trend exposed on a logarithmic Rb/Sr plot (Fig. 9a) is in good agreement with a fractionation of Cpx and Plag for the charnoenderbites. Bt can be ruled out as a fractionating phase from this diagram. Opx, which would cause a trend similar to the one caused by Cpx, may also have been a fractionating phase. On the logarithmic diagram of Ba/Sr (Fig. 9b) the trend defined by the Sarahuru charnoenderbites follow again the resulting vector of Plag, Cpx/Opx. We interpret the data points of the other NMZ charnoenderbites accordingly. The trend towards the retrogressed Sarahuru samples runs contrary to the fractionation vector of Kfs, and can be explained as an input of LIL-elements: advection of H_2O is required for the retrogression and it appears that the fluids carried LIL-elements. Partial melting of the charnoenderbites should form granites and charnockites with lower Ba and Sr (due to retention of Ap, Plag and Bt) and higher Rb (due to near 100% melting of Kfs-component) than the source, as a function of the fraction of partial melting. The trends for the Razi-type granites and charnockites behave in such a way. Some overlap of the trend of the granites and charnockites with that of the retrogressed samples is however also apparent. The Chilimanzi granites display in the Rb/Sr and Ba/Sr plots (Figs 9a–b) trends following fractionation of Kfs. Ni and Cr are compatible in Opx, Cpx and Ilm. The generally decreasing trend displayed in the logarithmic Ni/Cr diagram (Fig. 10) may be an indication of fractionation of Px and possibly Ilm which is a common phase in most of the NMZ charnoenderbites; its fractionation is further supported by the decrease of TiO_2 with increasing SiO_2 (Fig. 7d).

The logarithmic diagram of Nb vs Y (Fig. 11) displays a single array in which cratonic and NMZ lithologies fall, characterized by low Y and Nb contents. Y and Nb contents play a large role in empirical geotectonic discrimination diagrams (PEARCE et al., 1984), but as the validity of these for the Archean is in doubt (e.g., CONDIE, 1991) we avoid an interpretation based on them. Rather we note the similarity of the rocks from both provinces in this respect, with low Y–Nb characteristics typical for Archean TTG as described by MARTIN (1986).

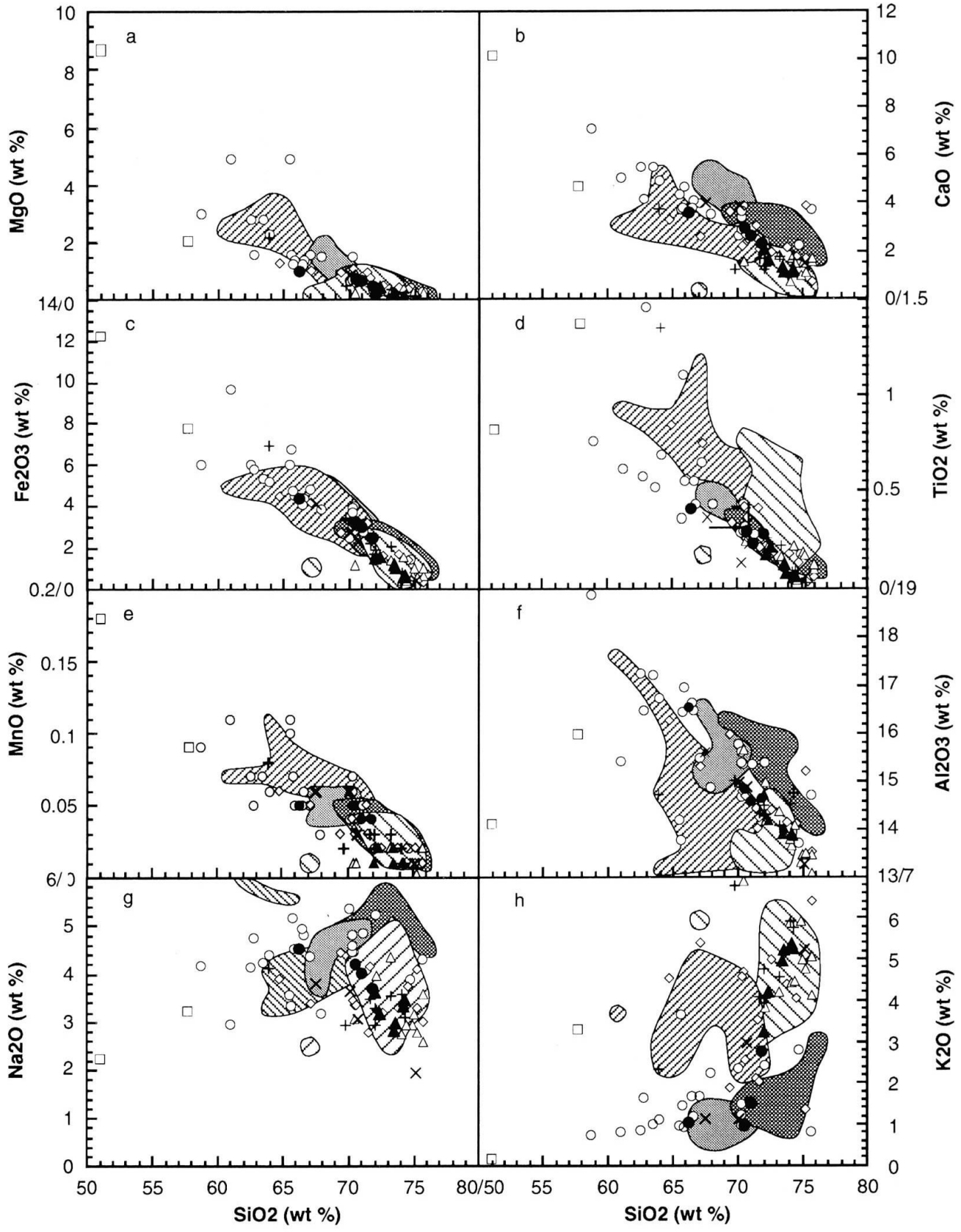

Fig. 7 a–h) Harker variation diagrams of MgO, CaO, Fe_2O_3, TiO_2, MnO, Al_2O_3, Na_2O and K_2O vs SiO_2 for the NMZ lithologies with 4 included lithologies from the ZC for comparison. Same symbols as in figure 6. For further explanation see text.

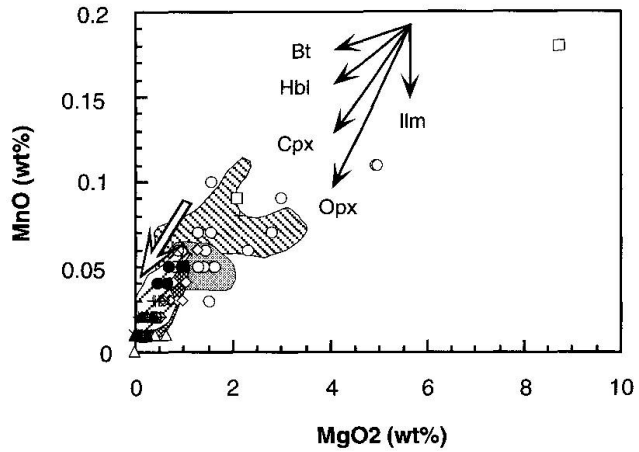

Fig. 8 Harker variation diagram of MnO vs MgO for the NMZ lithologies with 4 included lithologies from the ZC for comparison. Same symbols as in figure 6. Fractionation vectors are calculated using microprobe data on phases from NMZ lithologies. White arrow images trend for NMZ charnoenderbites. For further explanation see text.

SUMMARY OF GEOCHEMICAL INTERPRETATIONS

Hbl did not play a major role in the evolution of the charnoenderbite suite, as is demonstrated by the MnO–MgO plot (Fig. 8), whereas Cpx, Plag and probably Opx fractionation can consistently explain the major- and trace-element behaviour. The probable evolution in the Px-stability field hence supports not only the petrographic evidence that the charnoenderbites had at least magmatic precursors, it supports also their primary magmatic origin as charnoenderbites.

The geochemistry of the Razi Suite granites and charnockites can be successfully explained as resulting from partial melting of these rocks (in agreement with field observations [Fig. 4c]). The fractionation of Kfs, observed for the Chilimanzi granites from the craton (Figs 9a–b), which are supposedly related to the Razi granites (Robertson [1973b]), is not in contradiction to the partial melting hypothesis for the Razi granites. The production of the Razi granite magmas took place in more or less the same crustal level as where they finally crystallized. Therefore partial melting and not fractionation related features should dominate their geochemistry. If the Chilimanzi granite magma were produced in a similar way to the Razi granites, and at the same crustal levels, but, given a displacement along the Umlali thrust of ca. 5 km, migrated upward by this much, the resulting granites would be expected to display geochemical features attributed to fractionation processes. In most of the major-element vs silica diagrams the NMZ rocks plot between the trends of the individual cratonic suites (e.g., Al_2O_3/SiO_2, CaO/SiO_2 Fe_2O_3/SiO_2) and the cratonic rocks among themselves show greater variability than the NMZ suite in almost all plots. This is not an artefact related to a larger database (ZC: 75 samples, NMZ: 74 samples): it really demonstrates the chemical homogeneity of the NMZ suite.

Chingezi and Mashaba tonalites type II of the ZC are essentially indistinguishable from the charnoenderbites in many geochemical features suggesting similar genetic processes, and possibly sources, for these rocks. Chingezi and Mashaba tonalites type I and the Chinamora gneissic granites are different as they correlate with Hbl instead of Px fractionation (Fig. 8). Overall these

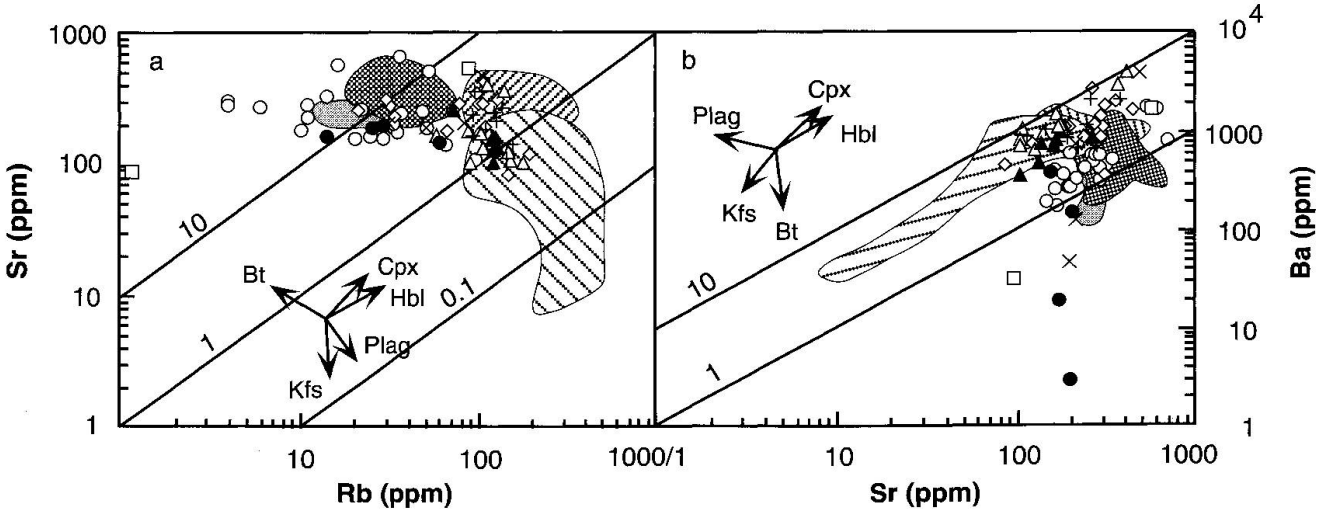

Fig. 9 a–b) Logarithmic trace-element variation diagrams for Sr–Rb and Ba–Sr for the NMZ lithologies with 4 included lithologies from the ZC for comparison. Fractionation vectors after Pearce and Norry (1979) and Atherton and Sanderson (1985). Same symbols as in figure 6. For further explanation see text.

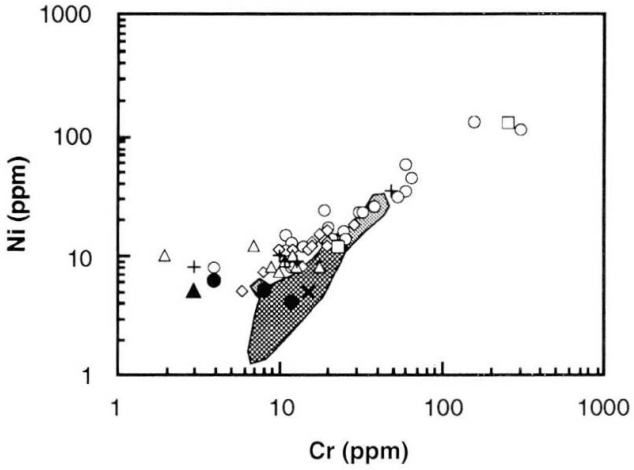

Fig. 10 Logarithmic trace-element variation diagram for Ni–Cr for the NMZ lithologies with 4 lithologies from the ZC included for comparison. Same symbols as in figure 6. For further explanation see text.

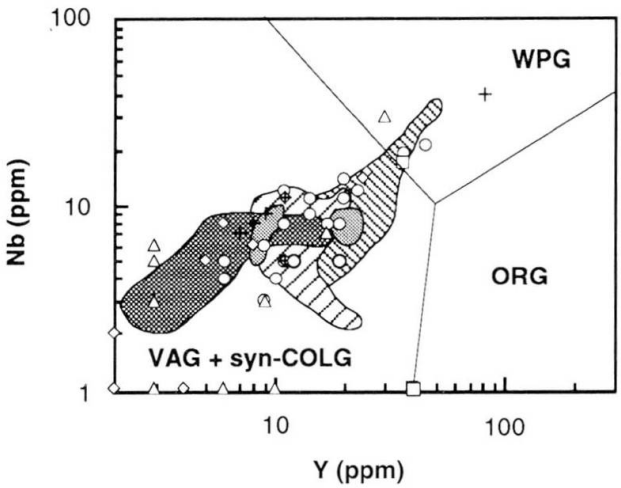

Fig. 11 Nb–Y geotectonic discrimination diagram (after PEARCE et al., 1984). Included are the NMZ lithologies and 4 lithologies from the ZC. Same symbols as in figure 6. Anorogenic tonalites and granites from the ZC mainly plot within the field of volcanic arc granites, alternatively they plot in the low Nb, low Y field, a characteristic of Archean anorogenic granites as described by CONDIE (1991). The NMZ lithologies show the same characteristics as the anorogenic cratonic rocks.

rocks also display trends similar to the ones of the respective NMZ rocks in major- and trace-element plots.

Geochronology

EXISTING AGE CONSTRAINTS

As mentioned in the introduction, only a few ages have been determined for the NMZ (HICKMAN, 1978; MKWELI et al., 1995), whereas the timing of the crust forming episodes in the Zimbabwe Craton is comparatively well constrained (e.g., HAWKESWORTH et al., 1975; MOORBATH et al., 1976, 1977, 1986; TAYLOR et al., 1991; JELSMA, 1993; VINYU, 1993). A short overview of the existing database for the southern ZC and the NMZ is provided in table 4.

SAMPLES

In this study, a total of 6 charnoenderbite samples were analyzed for U/Pb on zircon and whole-rock Sm/Nd. A seventh sample of charnoenderbite was only subjected to whole-rock Sm/Nd and an additional 3 whole-rock samples of Razi-type charnockites and granites were analyzed for Sm/Nd to test a possible partial-melting relationship of these rocks to the charnoenderbitic suite.

All samples were from batholith-like occurrences of charnoenderbites, with 4 samples having been affected by a weak deformation as is shown by the gneissic foliation.

Samples 90/78F and 90/78G are massive, dark green medium grained massive charnoenderbites from the Sarahuru quarry (Figs 2 and 3). Sample 90/79A is a dark grey-green medium grained charnoenderbite, from a road section on the Rutenga-Masvingo road south of the Runde River bridge (Fig. 2). In this area migmatization of the charnockites gives rise to garnetiferous leucosomes. Sample 92/050 is a medium grained dark grey-green enderbite with a weak gneissic foliation. It originates from a quarry at Bangala dam (Fig. 2) which was previously sampled by HICKMAN (1978, Tab. 4), who obtained a 2883 ± 47 Ma Rb/Sr errorchron from this locality. In the quarry a localized migmatization similar to the one noted in the sampling area of 90/79A was observed. The migmatization at Bangala dam quarry produced garnet bearing quartzo-feldspathic veins, but left some areas, up to 5 m wide, apparently unaffected. The enderbite sample 92/050 was from such an unaffected zone. A similar migmatization has been described by KAMBER et al. (1995) from the Triangle Shear Zone.

In the Mwenezi river section, north of Manyuchi dam, sample 92/111 was taken (Figs 2 and 3). The rock is a fine to medium grained dark green enderbite wich carries a faint gneissic texture. Sample 92/113, a medium grained dark green enderbite, originated from a quarry 2 km SW of Manyuchi dam (Figs 2 and 3). The samples analyzed for Sm–Nd only are 92/003, a medium to

coarse grained brownish grey enderbite, 92/013, a coarse grained brownish-grey porphyric charnockite, 92/014, a medium to coarse grained porphyritic charnockite and 93/508, a coarse grained porphyritic granite. Sample 92/003 was taken in the Tokwe river, samples 92/013–014 were taken in the northern part of the Mundi river profile, approximately 5 km south of the Umlali thrust (MKWELI et al., 1995) and sample 93/508 originated from the Samba Hills in the south eastern NMZ (Figs 2 and 3).

ANALYTICAL METHODS

U/Pb on multi Zircon-fractions

Zircon samples of 0.01–1.6 mg were digested in HF in Savilex® vessels which were enclosed in steel jacketed PTFE bombs, followed by Pb and U extraction in microcolumns with HBr and HCl. Samples were aliquoted and a ^{208}Pb–^{235}U mixed spike was used for concentration measurements. Pb was loaded on single Re filaments with H_3PO_4 and silica gel and was measured statically on a VG Sector ® fully automated 5 collector mass spectrometer. U was loaded on triple Ta–Re–Ta filaments and was measured on an Avco 90°, 350 mm radius single collector instrument. The values obtained on standard NBS 981 are, for the $^{207}Pb/^{206}Pb$ ratio, 0.91448 ± 0.00048, for $^{208}Pb/^{206}Pb$, 2.1648 ± 0.0020, and for $^{204}Pb/^{206}Pb$, 0.05916 ± 0.00004 (errors quoted are 1 s.d. of population of 85 measurements), and fractionation corrections were made accordingly. The lead blank of the total procedure varied between 90 and 110 pg during the time of analysis. Errors provided for the intercept ages are 2 σ errors.

Sm/Nd on whole-rock

Samples of 100 mg whole-rock powder were digested in HF in Savilex® screw top containers. Chemistry and measurement procedures followed the routine described by NÄGLER and FREI (in prep.). Sm and Nd measurements were made on the Avco single collecter mass spectrometer. Nd isotopic ratios were normalized to $^{146}Nd/^{144}Nd = 0.7129$. The mean value for the La Jolla standard during the period of mesurement was 0.511872 for $^{143}Nd/^{144}Nd$, with an 2 σ external reproducibility of ± 0.000025 (16 measurements).

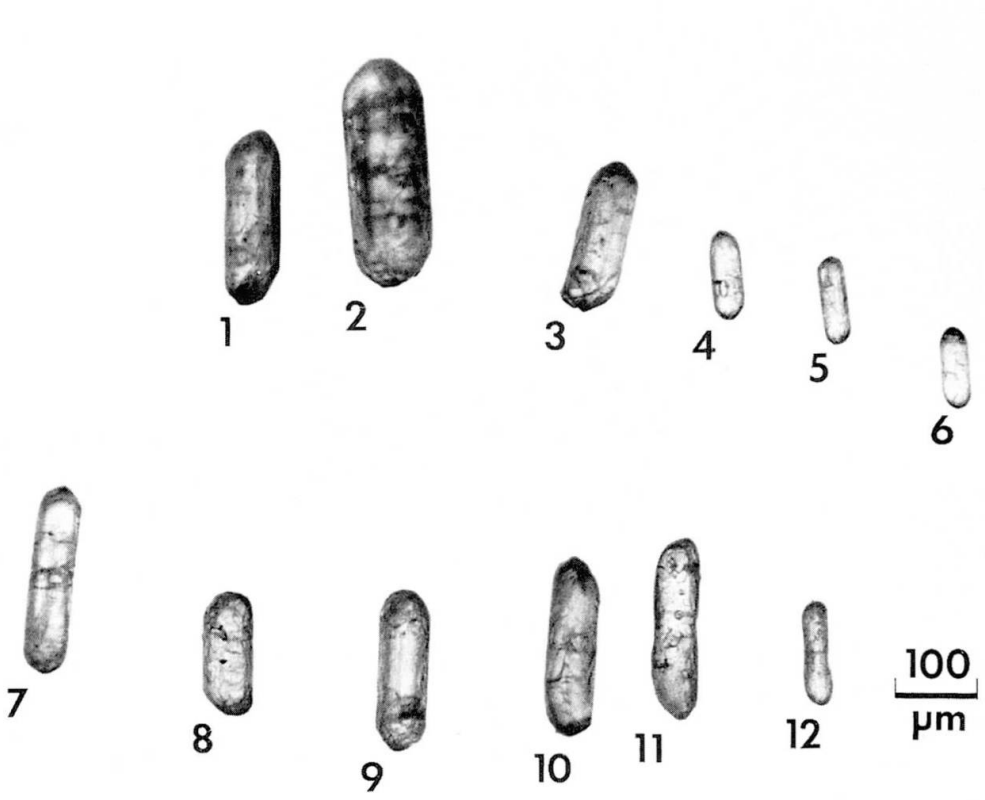

Fig. 12 Photograph of zircons from 4 charnoenderbite samples: 1–7: sample 92/113, 8: 90/79A, 9–10: 90/78G and 11–12: sample 92/111. For further explanation see text.

Tab. 2 U–Pb isotopic compositions of zircons from the NMZ.

Sample	Zircon fraction (mm)	Pb (ppm)	U (ppm)	$^{206}Pb/^{204}Pb$	$^{207}Pb^*/^{206}Pb^*$	$^{206}Pb^*/^{238}U$	1 SD ($^{206}Pb^*/^{238}U$)	$^{207}Pb^*/^{235}U$	1 SD ($^{207}Pb^*/^{235}U$)	discordancy (%)
90/78G	50–60	760.9	1728.3	4114	0.17716	0.40995	0.0007	10.01347	0.037	27
	70–80	677.3	1571	2327	0.17689	0.40427	0.0003	9.85998	0.011	28.8
	80–110	681	1634.4	2482	0.17538	0.39342	0.0005	9.51315	0.021	31.3
	110–165	571.2	1395.5	1823	0.17547	0.38936	0.001	9.42009	0.031	32.2
90/78F	30–60	641.8	1624.6	2667	0.17459	0.37176	0.0011	8.9493	0.032	40.8
	60–80	636.5	1750.4	1663	0.17154	0.34411	0.0014	8.13873	0.034	46.7
	80–110	881.3	2571.9	1340	0.16901	0.32533	0.003	7.58137	0.069	51.5
	110–165	797.7	2348.5	1159	0.16635	0.32299	0.0009	7.40844	0.021	52.7
	165–225	1073.2	3427.4	635	0.15727	0.30158	0.0027	6.53947	0.118	58.6
90/79A	30–50	776.9	2164.2	1235	0.16125	0.32345	0.0005	7.19121	0.014	29.7
	60–70	447.4	1343.7	1423	0.16043	0.29162	0.0001	6.45093	0.004	36.8
	70–80	549.5	1668.5	1298	0.15914	0.29495	0.0003	6.4718	0.006	36.5
	80–110	550.8	1615.5	1364	0.15955	0.30709	0.0002	6.75556	0.005	31.9
	110–165	879	2516.9	1416	0.15946	0.31626	0.0002	6.95327	0.005	33.8
92/111	30–50	570	1204.8	7994	0.17129	0.44209	0.0014	10.4411	0.034	13.7
	50–60	759.7	1693.7	7452	0.16924	0.41983	0.0015	9.79693	0.035	19.6
	140, lpr*	545.3	1216.9	876	0.1703	0.41684	0.0074	9.78754	0.183	24.8
	140, spr*	940.3	2173.5	778	0.16918	0.39645	0.0024	9.24761	0.06	20.2
92/113	50–60	580.5	1299.5	8525	0.17658	0.40182	0.0007	9.78293	0.019	22
	60–70	714.3	1303.3	14327	0.17716	0.49185	0.0014	12.01462	0.05	3.8
	70–80	366.2	1012.2	3818	0.17434	0.32644	0.0009	7.84709	0.033	37.7
	80–110	431.1	1266.9	3153	0.17332	0.30763	0.0008	7.35156	0.031	41.2
92/050	30–50	441.5	2072.3	704	0.12932	0.20125	0.0001	3.58831	0.004	45.2
	50–60	373.9	1806	861	0.13105	0.1961	0.0001	3.54347	0.003	46.2
	60–80	446.6	2172.8	667	0.1237	0.19443	0.0003	3.31628	0.006	49.2
	80–110	340.1	1818	462	0.12715	0.17403	0.0001	3.0509	0.003	53.5
	110–165	326	1736.3	536	0.12527	0.17498	0.0005	3.02227	0.01	53.8

Data corrected for blank and common lead. Pb 207/206 ratios have a 1 S.D. error of 0.1 % (0.00018); lpr: long prismatic, spr: short prismatic

RESULTS

U/Pb

Zircon populations of the charnoenderbitic samples are very similar with regard to their shape, size and colour. They consist of relatively clear, faintly brownish-grey coloured prismatic to long prismatic zircons that have round edges (Fig. 12). The zircons show signs of radiation damage and have minor inclusions of transparent and opaque minerals which are several microns in size (Fig. 12). However, no metamict zircons were observed in the samples except for the Bangala dam sample (92/050), which shows in addition to the type described above, a population of opaque prismatic zircons. The colour of these zircons varies from grey-white to yellowish-green and green. These zircons have been excluded from analysis. The U contents of the examined fractions varies between ca 1000 to 3500 ppm. Except for one near-concordant 60–70 μm zircon fraction of sample 92/113 all fractions had experienced lead losses that caused discordancies in the range of 14–59%. There is no systematic correlation, however, between the discordancy of a zircon fraction and their U-content /grain size. Abrading two zircon fractions of sample 92/050 to 70% of their original grain size had no effect on their discordancy. The lead loss that caused the apparent lower intercept ages therefore appears to have affected the whole grains. Comparison with zircon data from other Archean terrains shows that the ca 200–800 Ma apparent lower intercept ages are not uncommon (e.g., SARKAR et al., 1994; THORPE et al., 1992).

Zircon dating of enderbite sample 92/111 yielded an upper intercept age of 2603 ± 64 Ma with a lower intercept of 600 ± 588 Ma (Fig. 13a, Tab. 2). The upper intercept is interpreted as the intrusion age of the enderbite and the lower one as the result of quasi continuous lead loss. For the enderbite sample 92/113 from Manyuchi dam an upper intercept age of 2637 ± 19 Ma and an ap-

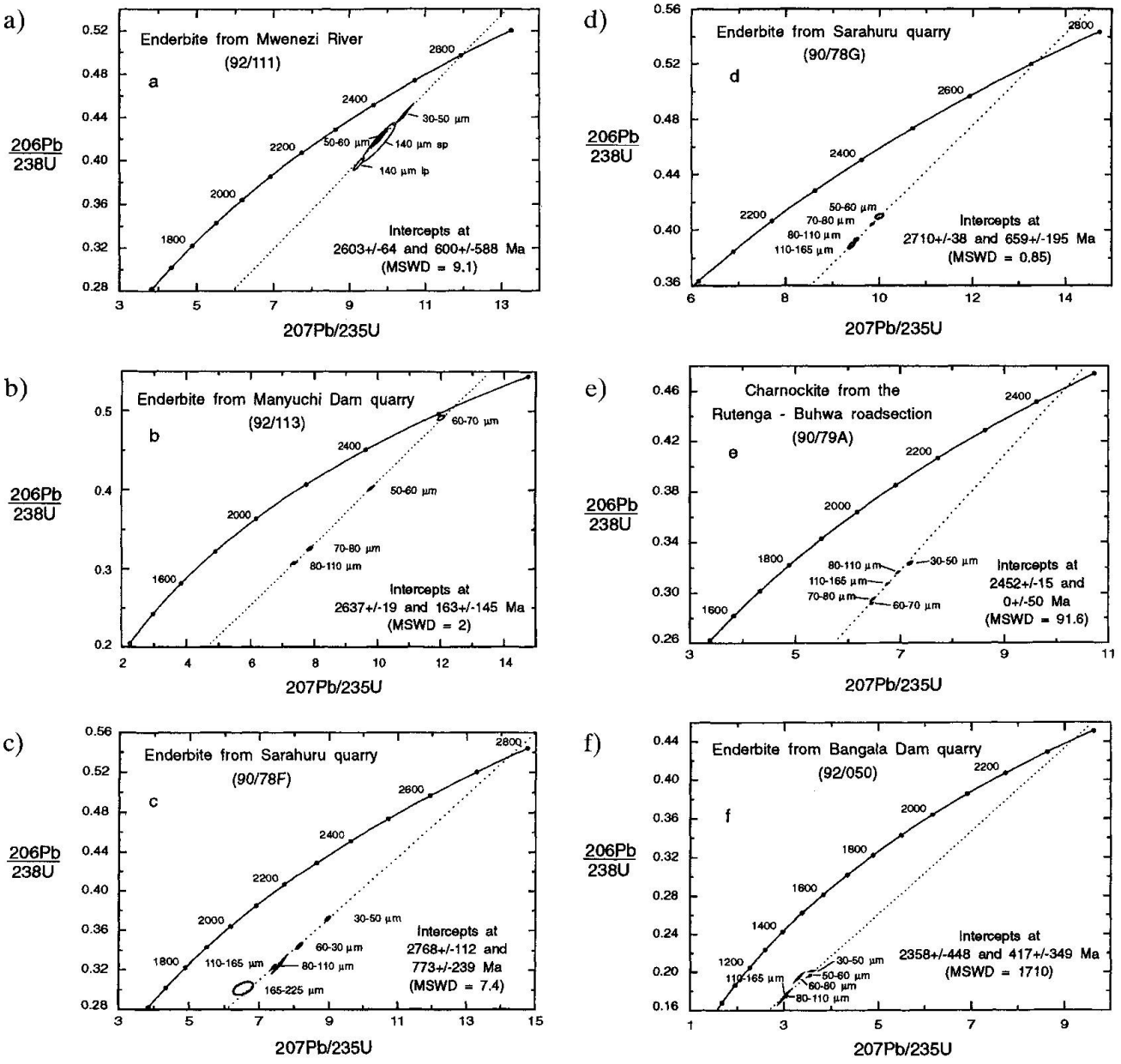

Fig. 13 a–f) Concordia diagrams of the charnoenderbite samples 92/111, 92/113, 90/78G, 90/78F, 90/79A, and 92/050.

parent lower intercept age of 163 ± 145 Ma (Fig. 13b, Tab. 2), which are interpreted in an analogous way. The two samples from Sarahuru quarry (90/78F and 90/78G) gave intercepts of 2768 ± 112 Ma and 773 ± 239 Ma and 2710 ± 38 Ma and 659 ± 195 Ma (Figs 13c–d, Tab. 2). We take the 2710 ± 38 Ma intercept age to be the intrusion age of the Sarahuru batholith, because it is also within error of the 2768 ± 112 Ma date of sample 90/78F. The lower intercepts are again considered geologically meaningless. Sample 90/79A would yield an upper intercept of 2452 ± 15 Ma by forcing the regression through zero (Fig. 13e, Tab. 2). Regressing the data without constraints additional to the data gives a negative lower intercept age, but a zero lower intercept lies within error. As previously mentioned, migmatization affected the sampling area of 90/79A. The 2452 ± 15 Ma intercept may hence reflect a partial (complete?) resetting of the U–Pb sytem rather than the intrusion age of this rock. The zircon fractions of sample 92/050 from Bangala dam quarry are highly discordant and scattered (Fig. 13f, Tab. 2). The discordia yields an upper intercept of 2358 ± 448 Ma and a lower intercept of 417 ± 349 with an MSWD of 1710. The scatter (high MSWD) may result from a combination of early episodic and quasi continuous lead loss; the first could be relat-

Tab. 3 Sm–Nd isotopic data on whole rocks of the NMZ.

Sample	Sm (ppm)	Nd (ppm)	$^{147}Sm/^{144}Nd$	$^{143}Nd/^{144}Nd$ 1)	2 σ_m	TDM (Ga) 2)	$\varepsilon_{Nd}0$ 3)
90/78F	3.23	20.43	0.0955	0.510752	± 11	3.08	–36.79
90/78G	5.21	29.53	0.1065	0.510938	± 23	3.13	–33.16
90/79A	7.06	43.01	0.0992	0.510881	± 7	3.00	–34.27
92/003	2.35	14.06	0.1009	0.510924	± 20	2.99	–33.44
92/050	5.52	27.18	0.1226	0.511314	± 16	3.06	–25.83
92/111	3.34	16.94	0.1192	0.511309	± 23	2.96	–25.92
92/113	5.09	31.33	0.0981	0.510829	± 12	3.05	–35.29
92/013	10.36	67.81	0.0924	0.510680	± 19	3.09	–38.20
93/508	21.85	131.61	0.1003	0.512095	± 17	3.03	–34.27
92/014	4.28	32.64	0.0793	0.510608	± 24	2.87	–39.60

1) The errors quoted are 2 σ_m of the respective analyses. For interpretation of the data the 2 σ reproducibility of standard analyses of ± 25 (referring to the last two digits) was used. Nd isotopic composition normalized to $^{146}Nd/^{144}Nd = 0.7219$.

2) Single step model (GOLDSTEIN et al., 1984).

3) ε_{Nd} – are derivations in parts per 10^4 from chondritic Nd at t = 0.

ed to the migmatization seen in the area. KAMBER et al. (1995) dated the high grade metamorphism in the nearby Triangle Shear Zone to be 2.0 Ga. In any case the apparent upper intercept age is not considered a significant date. It is in great contrast to the Rb–Sr whole rock errorchron date of 2883 ± 47 Ma obtained by HICKMAN (1978). The question arises, if the Rb–Sr system was also affected by the high grade thermal event that caused the observed migmatization. In the light of the three zircon dates between 2.6 and 2.71 Ga obtained on the other localities in the NMZ the Rb–Sr age seems to be too high, although it does not exceed the T_{DM}'s observed for the charnoenderbitic suite.

Sm/Nd

The Sm/Nd isotopic results obtained on the same samples as for the zircon-dating plus two Razi Suite samples are listed in table 3 and are shown on figure 14. $^{147}Sm/^{144}Nd$ ratios for all samples give a spread between 0.0793 and 0.1226. Following the suggestion of NÄGLER and STILLE (1993), the model of GOLDSTEIN et al. (1984) was used for the calculation of the Sm–Nd model ages. The obtained T_{DM} for the 6 charnoenderbite samples, 90/78f, 90/78G, 90/79A, 92/050, 92/111, 92/113 and the two Razi Suite charnockites 92/013 and 92/014 scatter closely around 3 Ga (2.9–3.1 Ga). Conspicuous is the very long gap of ca. 400 Ma, between the Nd model ages and the U–Pb ages.

DISCUSSION OF THE GEOCHRONOLOGICAL DATA

The isotope data obtained for the charnoenderbites document a series of intrusions in the time span between ca 2.71 Ga (and possibly older) and 2.6 Ga, where the youngest intrusions are coeval with the time of retrogression and the movement on the Umlali thrust (MKWELI et al., 1995). The Nd model ages of 3.1 to 2.9 Ga are quite homogeneous and in great contrast to the U–Pb ages of 2.71–2.6 giving differences of 360 to 420 Ma. Even T_{CHUR} ages are on average about 100 Ma older

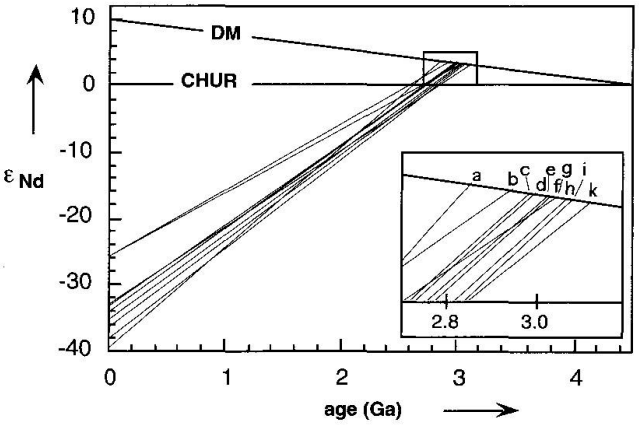

Fig. 14 Data for depleted mantle (DM) based on the model of GOLDSTEIN et al. (1984). Evolution lines of the charnoenderbites intercept the DM-evolution line in a well defined array between 2.96 and 3.13 Ga. Intercepts of the Razi Suite charnockites evolution lines with the DM-evolution line are 2.87 and 3.09 Ga. Signatures: a: 92/014, b: 92/111, c: 93/508 , d: 90/79A, e: 92/003, f: 92/113, g: 92/050, h: 90/78F, i: 92/013, k: 90/78G.

than the intrusion ages (Fig. 14). The question arises if all rocks of the suite are primarily of the same derivation age or if they have been homogenized later. The Nd model ages either reflect differentiation from the depleted mantle in a discrete crust forming event (= province age) at around 3.0 Ga, or may be interpreted as a subsequent extraction of melt from the depleted mantle coupled with the recycling of older crustal material. In the latter case a convective process must be responsible for the homogenization of originally isotopically different material.

A more uniformitarian view would be that of an Archean island arc setting. In that case the ε_{Nd} calculated for the intrusion age (for simplification 2.7 Ga for all samples are assumed here) should reflect the composition of the source. Present day intraoceanic arcs have Nd compositions 1 to 2 ε units below MORB (MORRIS and HART, 1983). The difference between today's MORB and CHUR is 10 ε units, whereas the difference between model depleted mantle and CHUR at 2.7 Ga is only 4 ε units. Correspondingly, the difference between intraoceanic island arc and depleted mantle at 2.7 Ga should be less than 1 ε unit, i.e. 40% of today's difference. Thus intraoceanic island arc material at 2.7 Ga can be assumed to have ε_{Nd} values around +3. This is in line with the compilation (n = 267) given by BLICHERT-TOFT and ALBAREDE (1994) of 2.7 Ga mafic rocks. 66% of these fall into the range of +1 to +5 ε units with a maximum around +3. Our data at 2.7 Ga, however range between +1 and –2 ε_{Nd}, significantly below such a supposed island arc source.

The T_{DM}'s obtained for the Razi Suite samples (2.9–3.1 Ga), are similar to those obtained for the charnoenderbitic suite. Together with the $^{87}Sr/^{86}Sr$ initial of 0.7047 ± 0.0007 obtained by MKWELI et al. (1995, Tab. 4, section Geological setting) on a Rb/Sr errorchron for retrogressive rocks and Razi-type granites and charnockites, which gives an apparent age of 2583 ± 52 Ma, this confirms the field observation that these rocks are probably reworked charnoenderbitic crust. An input of mantle derived material in variing quantities can not be excluded, especially as one T_{DM} is > .1 Ga lower than the charnoenderbite average of 3.0 Ga.

Conclusions

The NMZ charnoenderbite suite is of a primary magmatic origin. It consists of a succession of plutonic bodies that crystallized at middle crustal levels under granulite facies conditions (water undersaturated melts) in a time span between at least 2.71 Ga and 2.6 Ga.

Arguments for a primary magmatic character are: 1. magmatic contacts between charnockites and enderbites and between charnoenderbites and mafic xenoliths; 2. petrographic evidence recorded in the mafic xenoliths and schollen by the prograde replacement textures from Hbl to Opx, Cpx, Qtz and Mag; dehydration reaction textures which are absent in the charnoenderbites; 3. the consistence of the geochemical behaviour of major and trace elements with magmatic fractionation of the charnoenderbites in the Cpx-Opx stability field.

It is further suggested by the Sm–Nd data that the formation of the charnoenderbites involved a major component of crustal reworking. Remelting of enderbites resulted in the formation of the Razi-suite charnockites and granites.The differences in trace element behaviour (Rb/Sr, Ba/Sr) of Razi Suite and Chilimanzi Suite granites are interpreted to be a function of different distances between source region of the magma and intrusion level in the crust.

As discussed in the Geochemistry section, the element behaviour of the plutonic suites from both terrains are very similar with respect to a number of parameters. The overall similar geochemical characteristics of the Zimbabwe Craton and the NMZ can indicate that there is a relationship between the two. On a broader scale the ZC and the NMZ are chemically both granite-greenstone terrains with the two main differences that 1) the NMZ tonalites and granodiorites crystallized under granulite facies conditions whereas the tonalites and granodiorites of the Craton crystallized under amphibolite facies conditions and 2) we observe relatively few ultramafic-quartz-magnetite associations in the NMZ that are possibly "greenstone belt remnants" while greenstone belt successions occur widespread in the ZC. Except for the Tokwe segment, the granites and tonalites of the craton intruded successively between ca 3.0 Ga and 2.6 Ga (see Tab. 4). The most voluminous intrusions in the southern craton took place around 2.98 to ca 2.8 Ga and around 2.6 Ga (Chilimanzi Suite). The existing Sm–Nd model ages of the 2.98 to 2.8 Ga intrusions (e.g., Chingezi and Mashaba tonalites, Rhodesdale gneiss) are around 3.0 Ga (see Tab. 4), in the same range as the T_{DM} obtained for the NMZ charnoenderbites. A straightforward way to explain the differences as well as the similarities between ZC and NMZ is that the NMZ is a deeper section of the ZC as previously considered by ROBERTSON and DU TOIT (1981), though an overthickened portion of it. The possible causes for this overthickening have been speculated on by RIDLEY (1992).

Tab. 4 Compilation of age data from the Zimbabwe Craton and the two marginal zones of the Limpopo Belt.

	U–Pb	Pb–Pb	Sm–Nd (TDM)	Rb–Sr
Craton				
Tokwe Segment				
Tokwe gneiss		3475 + 97/–93 Ma: 12	3.64–3.68 Ga: 9	3500 ± 400 Ma: 1
Shabani gneiss		3088 + 44/–46 Ma: 12	3.36–3.55 Ga: 12	3495 ± 120 Ma: 4
Mushandike granodiorite		2917 ± 171 Ma: 12	3.62 Ga: 12	
		2946 + 125/–135 Ma: 12		
Mont d'Or tonalite		3345 ± 55 Ma: 8		3350 ± 120 Ma: 3
Mont d'Or granite			3.71–3.74 Ga: 12	
Mid-Archean				
Chingezi tonalite		2874 ± 32 Ma: 12	3.09–3.18 Ga: 12	2810 ± 70 Ma: 6
		2825 + 94/100 Ma:12		2818 ± 91 Ma: 12
		2800 + 7276 Ma: 12		2684 ± 102 Ma: 12
		2686 + 121/–133 Ma: 12		
Rhodesdale gneiss			3.11 Ga: 12	2700 ± 80 Ma: 4
Umwindisi gneiss				2865 ± 135 Ma: 10
Mashaba tonalite				2860 ± 60 Ma: 6
Late-Archean				
Somabula tonalite		2752 + 50/–52 Ma: 12	2.86 Ga: 12	2594 ± 80 Ma: 4
Sesombi tonalite		2579 + 154/–173 Ma: 12	2.81 Ga: 12	2633 ± 140 Ma: 1
Wedza Suite (Nyanji)	2667 ± 4 Ma: 14			2680 ± 104 Ma: 10
Black Cat porphyry	2672 ± 12 Ma: 14			
Jumbo granodiorite	2664 ± 6 Ma: 15			
Bindura granodiorite	2649 ± 9 Ma: 15			
Glendale tonalite	2618 ± 7 Ma: 15			
Chishawasha granodiorite		2646 + 37/–38 Ma: 15		2574 ± 14 Ma: 2
Chilimanzi Suite	2601 ± 14 Ma: 14			2570 ± 25 Ma: 5
Limpopo Belt				
NMZ				
charnoenderbites	2710 ± 38 Ma: 17		3.08–3.13 Ga: 17	
	2637 ± 19 Ma: 17		3.05 Ga: 17	
	2603 ± 64 Ma: 17		2.96 Ga: 17	
			3.06 Ga: 17	
			3.00 Ga: 17	
			2.99 Ga: 17	
				2883 ± 47 Ma: 5
Razi-type granites and	2627 ± 7 Ma: 16			2583 ± 7 Ma: 16
charnockites	2669 ± 67 Ma: 16		2.87–3.09 Ga: 17	
SMZ				
Matok pluton			3.23–3.30 Ga: 13	2620 ± 27 Ma: 7
				2603 ± 129 Ma: 7
Matok charnoenderbite	2671 ± 2 Ma: 13		3.15 Ga: 13	
enderbite	2715 ± 5 Ma: 11			
charnoenderbite			3.10–3.12 Ga: 13	

1 = HAWKESWORTH et al. (1975), 2 = HICKMAN (1976), 3 = MOORBATH et al. (1976), 4 = MOORBATH et al. (1977), 5 = HICKMAN (1978, recalculated for lamda = 1.42 x E-11 y E-1), 6 = HAWKESWORTH et al. (1979), 7 = BARTON et al. (1983), 8 = TAYLOR et al. (1984), 9 = MOORBATHET al. (1986), 10 = BALDOCK and EVANS (1988), 11 = RETIEF et al. (1990), 12 = TAYLOR et al. (1991), 13 = BARTON et al. (1992), 14 = JELSMA (1993), 15 = VINYU (1993), 16 = MKWELI et al. (1995), 17 = present study. All Nd-model ages are (re-)calculated for the model of GOLDSTEIN et al. (1984).

A continent-continent collision model is incompatible with the data for the following reasons: 1. the existence of a pure magmatic granulite suite with no evidence for tectonic contacts to the greenstone belt remnants; 2. the long time span of at least a 110 Ma of charnoenderbitic, granulite facies, intrusions ("metamorphic peak" in a tectonic model) followed by deformation at 2.6 Ga.

An Island arc setting can be excluded from consideration, as it could be shown that the Nd characteristics of the charnoenderbites do not correlate with the Nd characteristics of magmas which would be produced in a late Archaean island arc setting.

Terrane accretion models (e.g., ROLLINSON, 1993), are also unconvincing, as the designated terrane and the core (ZC), onto which it is supposed to have been accreted, do not differ in their geochemical properties and do not show sufficient differences in their geological histories.

A "soft" continent model (CHOUKROUNE et al. [in press]; RIDLEY and KRAMERS [1990]) is in broad agreement with our results, in the sense that the multiple intrusions of apparently well mixed, but older sialic material document near-solidus conditions in the lower to middle crust persisting for long periods (> 100 Ma) during the Archean.

Acknowledgements

The authors like to thank R. Armstrong, J. Ridley, H.R. Rollinson, and D. van Reenen for their helpful and constructive reviews. B. S. Kamber, T. Blenkinsop and S. Mkweli are thanked for fruitfull discussions on various aspects of Zimbabwe Craton and NMZ geology. R. Frei set up the U–Pb facilities in the isotope geology in Berne, and gave very helpful advices on zircon analyses.

Research was funded by the Swiss National Fonds, grant No. 20 33975.92.

References

ATHERTON, M.P. and SANDERSON, L.M. (1985): The chemical variation and evolution of the superunits of the segmented coastal batholith. In: Pitcher et al. (ed.). Magmatism at a plate edge: the peruvian Andes. Blackie, 208–227.

BALDOCK, J.W. and EVANS, J.A. (1988): Constrains on the age of the Bulawayan Group Metavolcanic Sequence, Harare Greenstone Belt, Zimbabwe. J. Afr. Earth Sci., 7, 795–804.

BARTON JR., J.M., FRIPP, R.E.P., HORROCKS, P. and MCLEAN, N. (1977): The geology, age and tectonic setting of the Messina Layered Intrusion, Limpopo Mobile Belt. Procedings of a seminar on the Limpopo Mobile Belt. Geol. Surv. Botswana Bull., 9.

BARTON JR., J. M., RYAN, B. and FRIPP, R.E.P. (1979): Effects of metamorphism on the Rb–Sr and U–Pb systematics of the Sigelele and Bulai gneisses, Limpopo mobile belt, southern Africa. Africa. Trans. Geol. Soc. S. Afr., 82, 259–269.

BARTON JR., J.M., DU TOIT, M.C., VAN REENEN, D.D. and RYAN, B. (1983): Geochronologic studies in the Southern Margina Zone of the Limpopo Mobile Belt, southern Africa. Geol. Soc. S. Afr. Spec. Publ., 8, 55–64.

BARTON JR., J. M., VAN REENEN, D.D. and ROERLNG, C. (1990): The significance of 3000 Ma granulite-facies mafic dykes in the central zone of the Limpopo Belt, southern Africa. Prec. Res., 48, 299–308.

BARTON JR., J.M., DOIG, R., SMITH, C.B., BOHLENDER, F. and VAN REENEN, D.D. (1992): Isotopic and REE characteristics of the intrusive charnoenderbite and enderbite geographically associated with the Matok Complex. Prec. Res., 55, 451–467.

BARTON JR., J.M., HOLZER, L., KAMBER, B., DOIG, R., KRAMERS, J.D. and NYFELER, D. (1994): We do not understand the Limpopo Belt: new data on the Bulai Batholith and the Metamorphism in the Southern Marginal Zone, Geology, 22, 1035–1038.

BLENKINSOP, T. and ROLLINSON, H. (1992): An Overview of the Limpopo Belt in Zimbabwe. North Limpopo Field Workshop, Zimbabwe.

BLICHERT-TOFT, J. and ALBAREDE, F. (1994): Short-Lived Chemical Heterogeneities in the Archean Mantle with Implications for Mantle Convection. Science, 263, 1593–1596.

BOHLEN, R.S., BOETTCHER, A.L., WALL, V.J. and CLEMENS, J.D. (1983): Stability of Phlogopite-Quartz and Sanidine-Quartz: A Model for Melting in the Lower Crust. Contrib. Mineral. Petrol., 83, 270–277.

BOHLENDER, F., VAN REENEN, D.D. and BARTON JR., J.M. (1992): Evidence for metamorphic and igneous charnockites in the Southern Marginal Zone of the Limpopo Belt. Prec. Res., 55, 429–449.

CHOUKROUNE, P., BOUHALLIER, H. and ARNDT, N.T. (in press): Soft Archean Lithosphere during periods of crustal growth or reworking. J. Geol. Soc. London.

CONDIE, K.C. (1991): Precambrian granulites and anorogenic granites: are they related? Prec. Res., 51, 161–172.

COWARD, M.P., JAMES, P.R. and WRIGHT, L. (1976): Northern margin of the Limpopo belt, southern Africa. Geol. Soc. of Amer. Bull., 87, 601–611.

COX, K.G., JOHNSON, R.L., MONKMAN, L.J., STILLMAN, C.J., VAIL, J.R. and WOOD, D.N. (1965): The geology of the Nuanetsi igneous province. Phil. Trans. R. Soc. London, A 257, 71–218.

DAVIES, R.D., ALLSOPP, H.L., ERLANK, A.J. and MANTON, W.I. (1970): Sr-isotopic studies on various layered mafic intrusions in southern Africa. Geol. Soc. S. Afr. Spec. Publ., 1, 576–593.

GOLDSTEIN, S.L., O'NIONS, R.K. and HAMILTON, P.J. (1984): A Sm–Nd isotopic study of atmospheric dusts and particulates from major river systems. Earth and planet. Sci. Lett., 70, 221–236.

HAWKESWORTH, C.J., MOORBATH, S., O'NIONS, R.K. and WILSON, J.F. (1975): Age relationships between greenstone belts and "granites" in the Rhodesian Archean Craton. Earth planet. Sci. Lett., 25, 251–262.

HICKMAN, M.H. (1978): Isotopic evidence for crustal reworking in the Rhodesian Archean Craton, southern Africa. Geology, 6, 214–216.

JAMES, P.R. (1975): A deformation study across the northern margin of the Limpopo Mobile Belt. Unpubl. Ph. D, Leeds.

JELSMA, H.A. (1993): Granites and Greenstones in Northern Zimbabwe: Tectono-thermal evolution and source regions. Unpubl. Ph. D. Thesis, Vrije Universiteit Amsterdam.

KAMBER, B.S., KRAMERS, J.D., NAPIER, R., CLIFF, R.A. and ROLLINSON, H.R. (1995): The Triangle Shear-zone, Zimbabwe, revisted: new data document an important event at 2.0 Ga in the Limpopo Belt. Prec. Res., 70, 191–213.

KRETZ, R. (1983): Symbols for rock-forming minerals. Amer. Mineral., 68, 277–279.

LUAIS, B. and HAWKESWORTH, H.J. (1994): The Generation of Continental Crust: An Integrated Study of Crust-Forming Processes in the Archean of Zimbabwe. J. Petrol., 35, 43–93.

MARTIN, H. (1986): Effects of steeper Archean geothermal gradient on geochemistry of subduction zone magmas. Geology 14, 753–756.

MASON, R. (1973): The Limpopo Mobile Belt – Southern Africa. Phil. Trans. R. Soc. London, A 273, 463–485.

MCCOURT, S. and VEARNCOMBE, J.R. (1992): Shear zones of the Limpopo Belt and adjacent granitoid-greenstone terranes: implications for late archean collision tectonics in southern Africa. Prec. Res., 55, 553–570.

MKWELI, S., KAMBER, B. and BERGER, M. (1995): Westward Continuation of the Craton-Limpopo Belt tectonic Break in Zimbabwe and new age constraints on the timing of the thrusting. J. geol. Soc. London, 152, 77–83.

MOORBATH, S., WILSON, J.F. and COTTERILL, P. (1976): Early Archean age for the Sebakwian group at Selukwe, Rhodesia. Nature, 264, 536–538.

MOORBATH, S., WILSON, J.F., GOODWIN, R. and HUMM, M. (1977): Further Rb–Sr age and isotope data on early and late Archean rocks from the Rhodesian Craton. Prec. Res., 5, 229–239.

MOORBATH, S., TAYLOR, P.N. and JONES, N.W. (1986): Dating the oldest terrestrial rocks: fact and fiction. Chem. Geol., 57, 63–86.

MORRIS, J.D. and HART, S.R. (1983): Isotopic and incompatible element constraints on the genesis of island arc volcanics from Cold Bay and Amak Island, Aleutians, and implications for mantle structure. Geochim. cosmochim. Acta, 47, 2015–2030.

NÄGLER, T.F. and FREI, R. (in prep.): Production of acidic rocks by pure differentiation of a depleted mantle source: a combined U–Pb-zircon, Pb–Pb–Nd isotope study on the Masirah Ophiolite, Oman.

NÄGLER, T.F. and STILLE, P. (1993): Remarks on depleted mantle evolution models used for Nd model age calculation. Schweiz. Mineral. Petrogr. Mitt., 73, 375–381.

ODELL, J. (1975): The geology of the country around Bangala dam. Geol. Surv. Rhodesia. Short Report, 42.

PEARCE, J.A. and NORRY, M.J. (1979): Petrogenetic Implications of Ti, Zr, Y, and Nb Variations in Volcanic Rocks. Contrib. Mineral. Petrol., 69, 33–47.

PEARCE, J.A., HARRIS, N.B.W. and TINDLE, A.G. (1984): Trace element discrimination diagrams for the tectonic interpretation of granitic rocks. J. Petrol., 25, 956–983.

RAITH, M. and SRIKANTAPPA, C. (1993): Arrested charnockite formation at Kottavattam, southern India. J. metamorphic Geol., 11, 815–832.

RETIEF, E.A., COMPSTON, E.A., ARMSTRONG, R.A. and WILLIAMS, I.S. (1990): Characteristics and preliminary U–Pb ages of zircons from Limpopo lithologies. Abstract Volume, Limpopo Workshop, Rand Afrikaans University, Johannesburg.

RIDLEY, J. (1992): On the origins and tectonic significance of the charnockite suite of the Archaean Limpopo Belt, Northern Marginal Zone, Zimbabwe. Prec. Res., 55, 407–427.

RIDLEY, J.R. and KRAMERS, J.D. (1990): The evolution and tectonic consequences of a tonalitic magma layer within Archean continents. Can. J. Earth Sci., 27, 219–228.

ROBERTSON, I.D.M. (1973a): The geology of the country Mount Towla, Gwanda district. Rhod. geol. Surv. Bull., 68.

ROBERTSON, I.D.M. (1973b): Potash granites of the southern edge of the Rhodesian Craton and the Northern Granulite Zone of the Limpopo Mobile Belt. Abstract volume 3, Symposium on granites, gneisses and related rocks.

ROBERTSON, I.D.M. and VAN BREEMEN, O. (1970): The Southern Satellite Dykes of the Great Dyke, Rhodesia. Geol. Soc. S. Afr. Spec. Publ., 1, 621–644.

ROBERTSON, I.D.M. and DU TOIT, M.C. (1981): Mobile belts. In: D.R. Hunter (ed.). The Precambrian of the southern Hemisphere. Elsevier, 641–671.

ROERING, C., VAN REENEN, D.D., SMIT, C.A., BARTON, J.M.J. (1992): Tectonic model for the evolution of the Limpopo Belt. Prec. Res., 55, 539–552.

ROLLINSON, H.R. (1993): A terrane interpretation of the Archean Limpopo Belt. Geol. Mag., 130, 755–765.

ROLLINSON, H.R. and BLENKINSOP, T. (1995): The magmatic, metamorphic and tectonic evolution of the Northern Marginal Zone of the Limpopo Belt in Zimbabwe. J. geol. Soc. London, 152, 65–75.

SARKAR, G., CORFU, F., PAUL, D.K., MCNAUGHTON, N.J., GUPTA, S.N. and BISHUI, P.K. (1993): Early Archean crust in Bastar Craton, Central India – a geochemical and isotopic study. Prec. Res., 62, 127–137.

SECK, H.A. (1971): Der Einfluss des Drucks auf die Zusammensetzung koexistierender Alkalifeldspäte und Plagioklase im System $NaAlSi_3O_8$–$KAlSi_3O_8$–$CaAl_2Si_2O_8$–H_2O. Contrib. Mineral. Petrol., 31, 67–86.

SNOWDEN, P.A. and SNOWDEN, D.V. (1981): Petrochemistry of the late archean granites of the Chinamora batholith, Zimbabwe. Prec. Res., 16, 103–129.

TAYLOR, P.N., KRAMERS, J.D., MOORBATH, S., WILSON, J.F., ORPEN, J.L. and MARTIN, A. (1991): Pb/Pb, Sm–Nd and Rb–Sr geochronology in the Archean Craton of Zimbabwe. Chem. Geol., 87, 175–196.

THORPE, R.I., HICKMANN, A.H., DAVIS, D.W., MORTENSEN, J.K. AND TRENDALL, A.F. (1992): U–Pb zircon geochronology of the Archean felsic units in the Marble Bar region, Pilbara Craton, Western Australia. Prec. Res., 56, 169–190.

TRELOAR, P.J., COWARD, M.P. and HARRIS, N.B.W. (1992): Himalayan-Tibetan analogies for the evolution of the Zimbabwe Craton and Limpopo Belt. Prec. Res., 55, 571–587.

VAN REENEN, D.D., ROERING, C., SMIT, C.A., VAN SCHALWYK, J.F. and BARTON JR., J.M. (1988): Evolution of the Northern High-Grade Margin of the Kaapvaal Craton, South Africa. J. Geol., 96, 549–560.

VAN REENEN, D.D., ROERING, C., BRANDL, G., SMIT, C.A. and BARTON JR., J.M. (1990): The granulite facies rocks of the Limpopo Belt, southern Africa. In: D. VIELZEUF and P. VIDAL (ed.). Granulites and Crustal Evolution. Kluwer, 257–289.

VINYU, M.L. (1993): Geochemistry and geochronology of the post-orogenic granitoids in the Harare-Sham-

va greenstone belt. Unpubl. Ph. D. Thesis, University of Zimbabwe.

WERNER, C.D. (1975): Saxonian granulites – igneous or lithogeneous. A contribution to the geochemical diagnosis of the original rocks in high-metamorphic complexes. In: H. GESTENBERGER (ed.). Contributions to the geology of the Saxonian granulite massif (Sächsisches Granulitgebirge). Zfl-Mitteilungen, 133, 221–250.

WILSON, J.F., BICKLE, M.J., HAWKESWORTH, C.J., MARTIN, A., NISBET, E.G. and ORPEN, J.L. (1978): Granite-greenstone terrains of the Rhodesian Archaean craton. Nature, 271, 23–27.

WINDLEY, B.F. (1993): Uniformitarianism today: plate tectonics is the key to the past. J. geol. Soc. London, 150, 7–19.

WORST, B.G. (1962): The Geology of the Buhwa Iron Ore Deposits and Adjoining Country. S. Rhod. geol. Surv. Bull., 53.

Manuscript received September 9, 1994; revision accepted January 23, 1995.